

# The role of snow processes and hillslopes on runoff generation in present and future climates in a recently constructed watershed in the Athabasca oil sands region

Kelly Biagi<sup>1</sup> and Sean Carey<sup>1</sup>

<sup>1</sup>McMaster University

May 26, 2020

## Abstract

Mine reclamation in the Athabasca oil sands region Canada, is required by law where companies must reconstruct disturbed landscapes into functioning ecosystems such as forests, wetlands and lakes that existed in the Boreal landscape prior to mining. Winter is a major hydrological factor in this region as snow covers the landscape for 5 to 6 months and is ~25% of the annual precipitation, yet few studies have explored the influence of winter processes on the hydrology of constructed watersheds. One year (2017-2018) of intensive snow hydrology measurements are supplemented with six years (2013-2018) of meteorological measurements from the constructed Sandhill Fen Watershed to: 1) understand snow accumulation and redistribution, snowmelt timing, rate and partitioning, 2) apply a physically-based model for simulating winter processes on hillslopes and 3) evaluate the impact of soil prescriptions and climate change projections on winter processes in reclaimed systems. The 2017-2018 snow season was between November and April and SWE ranged between 40-140 mm. Snow distribution was primarily influenced by topography with little influence of snow trapping from developing vegetation. Snow accumulation was most variable on hillslopes and redistribution was driven by slope position, with SWE greatest at the base of slopes and decreased towards crests. Snowmelt on hillslopes was controlled by slope aspect, as snow declined rapidly on west and south-facing slopes, compared to east and north-facing slopes. Unlike results previously reported on constructed uplands, snowmelt runoff from uplands was much less (~30%), highlighting the influence of different construction materials. Model simulations indicate that antecedent soil moisture and soil temperature have a large influence on partitioning snowmelt over a range of observed conditions. Under a warmer and wetter climate, average annual peak SWE and snow season duration could decline up to 52 % and up to 61 days, respectively while snowmelt runoff ceases completely under the warmest scenarios. Results suggest considerable future variability in snowmelt runoff from hillslopes, yet soil properties can be used to enhance vertical or lateral flows.

## 1. INTRODUCTION

Surface mining in the Athabasca oil sands region (AOSR) of northern Alberta, Canada, has disturbed >900 km<sup>2</sup> of forests and wetlands in the Western Boreal Plains (WBP), as entire landscapes are removed and excavated up to 75 m to access the bitumen-rich McMurray formation (Canada's Oil & Natural Gas Producers, 2017). These mining activities have permanently altered pre-disturbance vegetation communities, carbon storage capacity (Rooney, Bayley, & Schindler, 2012), soil layers (Nwaishi et al., 2015) and hydrologic functioning of these natural systems (Price, McLaren, & Rudolph, 2010; Rooney et al., 2012; Trites & Bayley, 2009). In addition to the physical disturbance, excessive salts are ubiquitous in the post-mining landscape from the tailings material that is used to backfill open pits (Biagi, Oswald, Nicholls, & Carey, 2019; Kessel, Ketcheson, & Price, 2018; Kessler, Barbour, van Rees, & Dobchuk, 2010; Simhayov et al., 2017). As part of their legal requirements, oil companies must reclaim disturbed landscapes into a mosaic of functioning ecosystems including wetlands, peatlands, forests and pit lakes (OSWWG, 2008) however, reclamation involves the complete reconstruction of these ecosystems, which is complicated given the regional sub-humid

climate, limited research and knowledge, ubiquitous salinity and the unprecedented scale of the disturbance (Daly et al., 2012; Elshorbagy, Jutla, Barbour, & Kells, 2005; Wytrykush, Vitt, Mckenna, & Vassov, 2012). Currently, only two watersheds that include peatlands have been constructed and instrumented which vary considerably in design (Daly et al., 2012; Ketcheson et al., 2016; Wytrykush et al., 2012).

The AOSR has a sub-humid climate which controls water availability primarily through precipitation and evapotranspiration (Devito, Mendoza, & Qualizza, 2012). Most of the annual precipitation in the WBP occurs during the growing season when evapotranspiration is highest, and excess of soil water is minimal (Ferone & Devito, 2004). Only ~25% of annual precipitation falls as snow (Environment Canada, 2019), yet snowmelt produces a large, but variable, surplus of water in a relatively short amount of time before the growing season when evapotranspiration is low (Devito, Creed, & Fraser, 2005; Devito et al., 2012). Autumn rainfall events and snowmelt are often the only source to replenish groundwater stores depleted by evapotranspiration during the previous growing season (Redding & Devito, 2011; Smerdon, Mendoza, & Devito, 2008). Additionally, snowmelt water is a critical source of freshwater to constructed watershed ecosystems that can have highly saline waters with elevated sodium concentrations which originate from the construction materials used in reclamation (Biagi et al., 2019). Winter processes therefore play an important role in reclamation hydrology as they influence snow storage, redistribution, melt and water transmission (Price, 1987; Price & Fitzgibbon, 1987; Rouse, 2000; Woo & Winter, 1993). Variations in blowing snow, sublimation, interception, frozen ground and vegetation communities among landscapes impact snow accumulation and melt regimes (Pomeroy et al., 2006, 1998; Price & Fitzgibbon, 1987; Spence & Woo, 2003; Whittington, Ketcheson, Price, Richardson, & Di Febo, 2012; Woo & Marsh, 2005; Woo & Winter, 1993). Soil ice formation is another critical component of winter hydrology as frozen soil water is unavailable in the early growing season for evapotranspiration (Devito et al., 2012; Van Huizen, Petrone, Price, Quinton, & Pomeroy, 2020). In addition, frozen ground can enhance snowmelt runoff to lowlands that may rely on this seasonal input of water prior to the growing season (Devito et al., 2012; Van Huizen et al., 2020).

Surface overland flow typically makes up a small component of the annual water balance in the undisturbed WBP due to the large storage capacity of soils even when frozen (Devito et al., 2005, 2012; Ferone & Devito, 2004; Redding & Devito, 2011). At the regional scale, a recent study reported that peatland-swamp ecosystems across the WBP are the primary producers of runoff (3 – 27 % of annual precipitation) and downgradient water transfer, while open-water wetlands and forestlands act as water sinks (Devito et al., 2017). Drivers of runoff generation are variable among WBP ecosystems and include snowpack depth (Devito et al., 2005; Ferone & Devito, 2004), concrete frost development (Redding & Devito, 2011), depth to confining layer and soil storage (Devito et al., 2005), snowmelt rate, autumn antecedent moisture conditions (Ireson et al., 2015; Redding & Devito, 2011) and to a lesser extent, vegetation canopy and soil type (Redding & Devito, 2011). Surface runoff also varies across the reclaimed landscape, where hillslopes with low antecedent soil water content and the presence of macropores only produces runoff once the high soil storage is exceeded (Kelln, Barbour, & Qualizza, 2009; Shurniak & Barbour, 2002), while hillslopes designed with a high antecedent soil moisture and low infiltration capacity (with finer textures) produces a high volume of surface runoff during snowmelt and heavy rain events (Ketcheson & Price, 2016b, 2016a). Soil materials used in reconstruction are harvested from the pre-mining landscape and can include coarse textured, fine textured and veneer-type soils, all of which represent different hydrologic response areas due to their unique soil properties (Devito et al., 2012). These soils are prescribed to reconstructed ecosystems based on desired hydrologic behaviour and storage capacity of the system and therefore construction practice can play a large role in dictating surface runoff from hillslopes in reclaimed watersheds in the AOSR (Kelln et al., 2009; Ketcheson & Price, 2016b; Shurniak & Barbour, 2002).

Modelling hydrological processes in constructed landscapes, particularly those that include wetlands, is

challenging because natural peatlands are complex heterogeneous systems that provide many key ecosystem functions and are resilient to change through feedback mechanisms (Waddington et al., 2014). Many studies have been successful at using models to highlight and explain hydrological processes observed in WBP, as well as potential ecosystem responses to disturbance or stress (Hilbert, Roulet, & Moore, 2000; Smerdon, Mendoza, & Devito, 2007; Thompson, Mendoza, Devito, & Petrone, 2015). Modelling constructed systems in the AOSR presents an additional challenge because of the dynamic nature of these systems within the first several years of development. There is no consistency of models used to represent constructed systems in the AOSR, as models have been chosen and developed to examine a specific process or operational questions. Of the models used, many have focussed on subsurface water fluxes (Carrera-Hernández, Smerdon, & Mendoza, 2012; Dobchuk, Shurniak, Barbour, Kane, & Song, 2013; Huang, Barbour, & Carey, 2015; Kelln, Barbour, & Qualizza, 2007; Kelln et al., 2009; Lukenbach et al., 2019; Shurniak & Barbour, 2002; Sutton & Price, 2019) and/or inorganic solute transport (Huang, Hilderman, & Barbour, 2015; Kelln, Barbour, & Qualizza, 2008; Kelln et al., 2009) with little focus on surface-atmosphere interactions, even though these are the dominant water fluxes in the WBP (Devito et al., 2012; Strilesky, Humphreys, & Carey, 2017). There are limited studies that focus on overall system performance that incorporate multiple components of the hydrological cycle in addition to subsurface processes (Elshorbagy et al., 2005; Elshorbagy, Jutla, & Kells, 2007; Keshta, Elshorbagy, & Carey, 2009), but few have been conducted on constructed peatlands or focus specifically on winter processes. An additional challenge in building landscapes in the AOSR is the uncertainty associated with climate change, as the WBP is expected to experience increases in temperature and precipitation in the coming century (Ireson et al., 2015; Meehl et al., 2007). We have a limited understanding of the role of climate change on constructed systems in the AOSR that already face challenges associated with water supply and quality. Such influences are not fully understood but are important for reclamation and closure plans as they could significantly impact the outcome of constructed systems in the long-term.

Constructed ecosystems provide a unique opportunity to study hydrologic functioning and development as these systems mature and develop in a continuously changing landscape and will likely differ considerably from their natural analogues (Elshorbagy et al., 2005). Despite the importance of winter processes, few studies (Kelln et al., 2009; Ketcheson & Price, 2016b; Meier & Barbour, 2002) have examined their influence on system hydrology of constructed watersheds in the AOSR. In addition, a range of soil prescriptions are used in reclamation and snowmelt partitioning will vary greatly depending on the soil properties which will influence water availability and down-gradient water transfer prior to the growing season. As up to 4800 km<sup>2</sup> of the AOSR is suitable for surface mining, understanding how winter processes influence system hydrology and water availability is critical for the long-term success of current and future constructed ecosystems. To address this, the objectives of this research are to use data from a constructed upland-wetland watershed to: 1) quantify snow accumulation and redistribution, melt timing, rate and partitioning, 2) apply a widely used physically-based model for simulating winter processes and runoff generation on upland hillslopes, and 3) evaluate the impact of different reclamation soils and climate projections on winter processes. This information will help guide future landscape construction practice and provide information on the potential long-term importance of winter processes in a changing climate.

## 2. SANDHILL FEN WATERSHED

The Sandhill Fen Watershed (SFW) is a constructed peatland-upland system in the northwest corner of East-In-Pit, a previously mined area (1977-1999), and is part of Syncrude Canada Ltd.'s Base Mine (57°02'N, 111°35'W) which is approximately 42 km north of Fort McMurray, Alberta. This region is situated in the Western Boreal Plains ecoregion of western Canada which is characterized by a cold and sub-humid climate where mean annual potential evapotranspiration (607 mm) is greater than mean annual precipitation (456 mm) (Environment Canada, 2019). Climate normals (1971 – 2010) for the Fort McMurray Airport indicates that most of the annual precipitation falls as rain (342 mm) and the remainder falls as snow (113 mm of water equivalent) with a regional average peak snow depth of 31 cm (February). Winter temperatures are typically coldest in January averaging  $-17.4 \pm 5$  @C and averages  $-12.1$  °C from November to March. The annual mean temperature is  $1 \pm 1.3$  @C (Environment Canada, 2019).

Over the course of four years (2009 – 2012), East-In-Pit was filled with 35 m of inter-bedded composite tailings and tailings sand layers followed by a 10 m tailings sand structural cap as part of the reclamation strategy. The SFW was then constructed on top of these materials and is 52 ha total with a 17 ha fen wetland, 35 ha upland including 20 ha of upland hillslopes (referred to as hummocks) (Wytrykush et al., 2012). Due to the relatively low grade of the wetland and upland areas, (0.1-0.5 %), the hummocks were constructed to create distinct groundwater recharge areas as well as add topographic variation to the watershed. The hummocks were constructed of tailings sand that was mechanically placed and capped with Pleistocene fluvial sand (see Table 1 for specific soil properties). A peat-mineral mix was placed in the lower upland areas while 0.5 m of clay followed by 0.5 m of donor peat materials were placed in the wetland area. Details of watershed design, construction materials and soil stratigraphy are outlined in Biagi et al. (2019). The SFW was vegetated in 2011 with species native to this region (Nicholls, Carey, Humphreys, Clark, & Drewitt, 2016; Wytrykush et al., 2012), but species composition has changed considerably throughout the watershed with time (Vitt, House, & Hartsock, 2016). Unique to the SFW, inflow and outflow can be managed via a pump system that was installed during construction. Fresh water can be supplied to the Water Storage Pond (Figure 1) from a near-by natural lake (Mildred Lake) which flows westward through the wetland area towards the outlet where water can be pumped out of the SFW and back into East-In-Pit. It should be noted that aside from deeper groundwater flow paths, the outflow of surface and near-surface water can only occur when the outflow pump is activated. The intention of these pumps was to mitigate the elevated salinity levels from construction materials by providing fresh water and flushing out saline water in the first few years while the system established within the disturbed landscape. These pumps have remained largely off since 2013 (Biagi et al., 2019; Nicholls et al., 2016).

### 3. METHODS

#### 3.1 Meteorological Measurements

Air temperature, windspeed and direction, relative humidity, short, and long-wave radiation were measured at each of the three meteorological towers (Figure 1) on SFW. Instrument details can be found in Nicholls et al., (2016). Precipitation was measured with a tipping bucket rain gauge (Model CS700, Campbell Scientific Inc. (CSI), Logan UT, USA) for rainfall, a CSI *CS725* to measure snow water equivalent (SWE) as well as a CSI SR50A sonic ranger to monitor snow depth. All measurements were recorded on an hourly basis with CSI CR1000 data loggers since 2013. In addition, one eddy covariance tower that was instrumented in 2013 measured turbulent fluxes year-round (Clark, Humphreys, & Carey, 2019; Nicholls et al., 2016).

#### 3.2 Snow Accumulation and Melt Measurements

Intensive field measurements were made during the 2018 winter season (November 2017 – April 2018) and included snow survey transects starting on 15 February 2018 throughout the different landscape units within SFW including the wetland, uplands and hummocks (Figure 1). Snow survey measurements included snowpack depth every 10 m using an avalanche probe, snow water equivalent (SWE) every 30 m using a Mount Rose corer and ground ice presence every 30 m using a metal rod. To supplement SWE measurements, snow pits were completed in the upland and wetland to quantify snowpack density using standard approaches. SWE measurements on the hummocks were divided into slope position and aspect to assess differences in snow accumulation patterns. Slope position was assigned using visual observations and contour lines where the bottom slope was within the first meter of the hillslope, the crest was the entire flat portion at the top and mid-slope was the remainder of the hillslope area in between. Slope aspect was assigned using the Aspect tool in the Spatial Analyst toolbox in ArcGIS. All statistical analysis of snow accumulation trends was completed using the R language for statistical computing (R Core Team, 2018).

To quantify and partition snowmelt from hummock hillslopes, surface runoff collectors were constructed

on the north- and south-facing slopes that drained into v-notch bucket weirs with a pressure transducer. Runoff collectors, modified from Ketcheson and Price (2016b), were constructed prior to melt by digging shallow trenches (~15 cm) that extended out from a bucket weir in a “V” shape where each arm of the “V” was approximately 3-4 m. Flexible, plastic garden edging was sealed into the bottom of the shallow trenches using hydraulic cement to ensure meltwater could not flow across the trenches. At the base of the “V”, a plastic eavestrough was used to direct surface runoff into the bucket weirs and was also sealed with hydraulic cement to limit leakage (Figure 2). Large patches of ground that were cleared for runoff collector construction were filled with snow after construction was completed to limit any change to ground surface albedo. A pressure transducer was installed in each bucket weir to continuously measure water level and discharge during melt. Discharge measurements for each bucket weir were made to create independent rating curves for each runoff collector. A one-meter resolution LiDAR digital elevation model (DEM) of the study area was used to determine the drainage direction and delineate the contributing area for each runoff collector using the Hydrology toolset in ArcGIS. Calculated contributing areas of runoff collector one (RC1) and two (RC2) were 331 m<sup>2</sup> and 160 m<sup>2</sup>, respectively (Figure 1). The horizontal and vertical accuracy of the LiDAR data was 30 cm and 15 cm, respectively at 95% confidence through comparison to independently surveyed ground points.

Snow surveys were also completed on older reclaimed sites on the Syncrude Canada Ltd. property that are in more advanced stages of regrowth to compare snow accumulation and melt patterns using the same methods as above. Sites were within 5 km from the SFW and included two mature reclaimed forests, South Bison Hill (~20-year-old mature aspen/white spruce stand) and Jack Pine (~30-year-old jack pine stand) have delayed melt compared with the newly reclaimed Coke Beach site (~10-year young aspen) and the SFW (~6 years).

### *3.3 Soil parameters*

Soil properties of hummocks have been measured as part of the active research at the SFW (2012 – 2018) and are summarized in Table 1. Both in-situ field and laboratory methods were used to estimate soil properties. Soil pits were constructed on hummocks to collect samples at various depths to capture all soil materials used in hummock construction. Saturated hydraulic conductivity (Ksat) values are averaged values from several data collection methods including in-situ using the Guelph Permeameter and single ring infiltrometer as well as laboratory methods using the KSAT and Hyprop instruments from METER Group Inc. Ksat estimation from the Guelph Permeameter followed standard procedures (Soilmoisture Equipment Corp., 2012). Single ring infiltrometers were used to estimate field Ksat and infiltration capacity. Single ring infiltrometers were installed into the ground surface to depths of at least 1 cm and constant head tests were conducted until a steady state infiltration rate was reached. Ksat was assumed to be equal to the steady state infiltration capacity reached during each test. Porosity is automatically calculated using the Hyprop software and specific yield can be estimated from the Hyprop data by the difference between the saturated volumetric water content (VWC) and the VWC at 330 mb which is equivalent to the field capacity of the sample. Samples were analyzed for bulk density using standard methods (Freeze & Cherry, 1979) with the exception that the samples were oven-dried at 80 °C to limit any loss of organic matter. Organic matter content was determined via loss on ignition (LOI) where samples were placed in a muffle furnace at 550 °C for four hours. LOI was calculated as the difference between the pre- and post-muffle furnace weight divided by the pre-muffle furnace weight. The remainder of soil properties in Table 1 were extracted from NorthWind Land Resources Inc. (2012).

### *3.4 Model setup and parameterization*

The cold regions hydrological model (CRHM) (outlined in Pomeroy et al., 2007) provides a platform to assess potential hydrological responses of constructed peatlands in the AOSR as it continues to develop and

in response to future climate change. CRHM is a physically based hydrological model that can simulate hydrological processes in a modular fashion and is particularly strong in representing winter hydrological processes (Pomeroy et al., 2007). Modules within CRHM are selected by the user based on what simulated processes are needed which cover a wide range of hydrological processes. CRHM can assign linked algorithms that simulate hydrological processes to different hydrological response units (HRUs) and can route water between HRUs through pathways such as blowing snow, overland flow, groundwater flow when specific thresholds for that unit are exceeded. This unique feature allows HRUs to be a series of cascades across the landscape (Pomeroy et al., 2007; Rasouli, Pomeroy, Janowicz, Carey, & Williams, 2014). Because CRHM is physically based and is a purpose-built model based on process understanding, typical calibration methods used in many other models are omitted. Divergence between model and observations are diagnosed based on process understanding and model structures changed until suitable dynamics are achieved (Cordeiro, Wilson, Vanrobaeys, Pomeroy, & Fang, 2017; Rasouli, Pomeroy, & Whitfield, 2019). CRHM has been successfully applied to a variety of catchments including the Canadian Prairies (Fang & Pomeroy, 2007, 2010; Fang et al., 2010; Shook, Pomeroy, Spence, & Boychuk, 2013), agricultural catchments (Cordeiro et al., 2017), arctic regions (Krogh & Pomeroy, 2018; Quinton & Baltzer, 2013; Quinton, Bemrose, Zhang, & Carey, 2009; Quinton, Carey, & Goeller, 2004), peatlands (Knox, Carey, & Humphreys, 2012; Quinton & Baltzer, 2013), and mountainous regions (Ellis, Pomeroy, Brown, & MacDonald, 2010; Fang et al., 2013; Pomeroy, Fang, & Ellis, 2012; Weber et al., 2016).

Several physically based modules were used (detailed in Pomeroy et al. (2012) and Fang et al. (2013)) to examine the hydrological controls on winter processes in the SFW and include the following:

1. Observation module: imports and reads observed meteorological data which include continuous, hourly time-steps of air temperature, precipitation, relative humidity, wind speed, incoming short-wave radiation and incoming longwave radiation which are used as forcing data to drive other CRHM modules.
2. Radiation module: global radiation, direct and diffuse shortwave radiation based on site latitude, elevation, slope and azimuth (Garnier & Ohmura, 1970). Radiation from this module is used in the sunshine hour module, energy budget snowmelt module and net all-wave radiation module.
3. Sunshine hour module: used shortwave radiation and maximum sunshine hours to estimate total sunshine hour. Estimates from this module are used in the energy-budget snowmelt module and et all-wave radiation module.
4. Slope correction for the shortwave radiation module: the incoming shortwave radiation at a level surface to estimate the incident shortwave radiation on a slope. The module uses the measured incoming shortwave radiation from the observation module as well as the calculated direct and diffuse solar radiation from the radiation module to calculate the adjustment ratio for the shortwave radiation on a slope.
5. Longwave radiation module: uses the measured shortwave radiation to estimate incoming longwave radiation (Sicart, Pomeroy, Essery, & Bewley, 2006), which is used in the energy-balance snowmelt module.
6. Albedo module: snow albedo is estimated for the duration of winter as well as the melt period. This module also indicated the beginning of melt which is used in the energy-balance snowmelt module.
7. SnobalCRHM: designed for deep alpine snowpacks (Marks, Domingo, Susong, Link, & Garen, 1999), SnobalCRHM simulates the mass and energy balance of the snowpack to estimate snowmelt by calculating the energy balance of radiation, sensible and latent heat, ground heat flux, advection from rainfall and change in internal energy for two layers of the snowpack (an active top layer and a lower layer).
8. frozenAyers: uses Ayers (1959) infiltration to estimate unfrozen soil infiltration and Zhao & Gray (1999) to estimate frozen soil infiltration and subsequent surface runoff. The soil moisture balance module is linked to both infiltration algorithms. Surface runoff occurs when snowmelt or rainfall exceeds the infiltration rate.

CRHM was initially set up for the 2018 winter season using detailed observations outlined above as one hummock HRU to evaluate snow accumulation and movement of meltwater from hillslopes to the lowlands. The lowlands were not simulated. Parameters were selected from direct observation where possible, and a suitable model performance was obtained (Table 2). CRHM was then run for the five previous years of observation to provide simulations for five winters under current climate conditions (T0-P1). Following this, CRHM was used to evaluate the potential impacts of climate change on these five years. Nine future climate scenarios for the WBP were selected from the Intergovernmental Panel on Climate Change report (Meehl et al., 2007) and applied to CRHM in a delta-change approach though systematically changing temperature, precipitation, and both, based on ensemble averages. In CRHM, temperature is an additive change while precipitation is a multiplicative change that only affects days with existing precipitation (a value of 1 represents current precipitation conditions). Model results are grouped based on increases in temperature (T) and precipitation (P) from their baseline temperature (0 °C), and precipitation (a value of 1 indicates no change in precipitation). First, air temperature was increased for 5 years of winter simulation by 2, 4 and 6 °C (T2-P1, T4-P1 and T6-P1, respectively). Second, under current temperature, days with precipitation had volume increases by factors of 1.15, 1.2 and 1.3 (T0-P1.15, T0-P1.2 and T0-P1.3, respectively), based on the IPCC predicted range of increased future precipitation (Meehl et al., 2007). Finally, to assess the impacts of both a warmer and wetter future, precipitation was increased by a factor of 1.2 in addition to the three temperature change scenarios (T2-P1.2, T4-P1.2 and T6-P1.2). CRHM was also used to test the influence of different soil parameters on the partitioning of snowmelt (under current climate conditions only). Soil parameters within the frozenAyers module that were evaluated were soil temperature at the onset of snowmelt in the top 40 cm, the initial soil saturation (VWC/porosity), and soil texture. Values were taken from the observed variability in the six years of data and directly measured soil physical properties.

## 4. RESULTS

### 4.1 Snow accumulation and distribution

The average peak watershed SWE was  $89 \pm 17$  mm ( $n=278$ ) during the 2017-2018 winter season with small but significant differences among landscape units determined by a simple Wilcoxon rank sum test. The wetland, uplands and hummocks had average peak SWE of  $94 \pm 13$  mm,  $90 \pm 16$  mm and  $85 \pm 20$  mm, respectively (Figure 3a), where the hummocks exhibited the most variability as a result of slope position and aspect (Figure 3b). Only the hummocks and uplands were statistically similar to one another ( $p=0.07$ ). The smallest snowpack was observed on the crest of the hummocks ( $71 \pm 16$  mm), followed by the mid-slope ( $88 \pm 17$  mm) and lower-slope ( $94 \pm 26$  mm) positions. The crest was significantly different than the mid and lower-slope positions ( $p<0.05$ ) while the mid and lower slopes were similar ( $p=0.3$ ). SWE accumulation and distribution were statistically similar among aspects ( $p>0.05$ ) except between north and east-facing slopes ( $p=0.04$ ). Average SWE on south-, east-, north- and west-facing slopes averaged  $91 \pm 22$  mm,  $99 \pm 17$  mm,  $84 \pm 17$  mm and  $90 \pm 17$  mm, respectively.

### 4.2 Snowmelt and Melt Partitioning

The SWE of all landscape units remained relatively stable until 12 March when SWE began declining during the first melt event which continued to decline to mid-April when the second (and final) melt event depleted the remainder of the snowpack (Figure 4). SWE decline was similar among all sites until the first melt event on 12-15 March. Once this melt started in mid-March, the hummock SWE was the most variable (Figure 4c) as melt among aspects was considerably different, where the south and west-facing slopes had faster melt rates than the north and east-facing slopes (Figure 4d). West-facing slopes had the largest SWE decline of ~25 mm whereas all other sites had a SWE decline [?] 10 mm. While no snow surveys were conducted between 15-March and 9-April, SWE decline was the largest during this time period for all sites which can be attributed to the warmer temperatures in mid-April as temperatures remained well below zero for the remainder of March. The second melt event began mid-April when air temperatures were above zero during

most days. The snowpacks on the south and west-facing slopes lost the majority of SWE by the second melt event in April whereas the remainder of the sites had approximately half of their snowpack left during the second melt event (12-24 April) (Figure 4).

To evaluate meltwater partitioning from hillslopes to the wetland area, two runoff collectors were constructed on the north- and south- and facing slopes (Figure 1). Snowmelt on the north-facing slope was not measured in March as it was not fully constructed however, the snowpack stayed deep and experienced minimal melt during the mid-March warm period. Snowmelt began on the south-facing slope on 15 March, with instantaneous discharge peaking the next day at  $\sim 190 \text{ cm}^3/\text{s}$  and total cumulative runoff reaching 10 mm in two days (Figure 5a). Following this, runoff occurred from the south-facing slope for the next five days between  $\sim 10:30\text{-}17:30$  each day and in total 15 mm was collected before this hillslope was snow-free on 23 March. In contrast, the north-facing slope did not begin to generate runoff until daily air temperatures were consistently near zero in mid-April. Snowmelt began on 12 April with peak instantaneous discharge of  $79 \text{ cm}^3/\text{s}$  on 14 April (Figure 5b). The first several days of melt were the most productive, yielding between 2 and 5 mm over the first four days with a shorter duration of daily melt (typically four hours in duration through mid-day). Runoff then declined as the slope became gradually snow-free by 24 April and yielded a total of 23 mm for the entire period. While there were no runoff collectors for upland sites, on-site observations confirm that surface runoff was only generated from hummocks as opposed to low-gradient areas surrounding the lowland.

The average SWE on the south- and north-facing slope prior to melt was 50 mm and 90 mm, respectively and total surface runoff totaled 15 mm and 23 mm, respectively and their corresponding runoff ratios were 0.31 and 0.26, respectively. Sublimation during the two melt periods was calculated from the eddy-covariance derived latent heat data and amounted to 0.44 mm from 15-21 March (south-facing melt) and 2 mm from 12-24 April (north-facing melt). Infiltration into the frozen ground was calculated as the residual after accounting for runoff and sublimation which was 34 mm and 65 mm for the south- and north-facing slopes, respectively. When all hillslopes feeding the wetland are considered and measurements are scaled, snowmelt surface runoff contributed  $\sim 11$  mm to the wetland area of SFW.

### 4.3 Model Simulation

#### 4.3.1 Influence of soil parameters on snowmelt partitioning.

To evaluate the role of soil properties and antecedent conditions on runoff generation from the hummocks, parameters within the frozenAyers module, which is derived from the parametric equations of heat and mass transfer in Zhao and Gray (1999), were adjusted based on field and laboratory observations. While the sensitivity of melt partitioning largely reflects parameter assignments in the model equations, it provides guidance on the expected influence of soil conditions on runoff generation from hillslopes based on the ranges of observed values.

Three key parameters that influence frozen soil infiltration are soil texture, the degree of initial soil saturation and ground temperature. Soil texture is important in a reclamation context as different textures are used in various landforms which will eventually be integrated into the closure landscape. The influence of texture on the partitioning of snowmelt is complex as liquid and frozen water influence capillary pressure and permeability. There also exists a relation between texture and soil temperature due to unfrozen water content and latent heat effects. Soil texture was changed within CRHM to silt and clay from the base 2018 winter simulation (sand, 34 mm of runoff). As expected, finer soil texture resulted in greater runoff, with silt loam (37 mm) and clay (41 mm) being 8 and 17 % greater than sand, respectively. It is important to note

that degree of soil saturation was not adjusted ( $S_i=0.2$ ), and changes in runoff are from textural differences alone. However, it is expected that finer textured soils would have greater antecedent wetness and therefore greater runoff.

The degree of initial soil saturation ( $S_i$ ), the upper soil volumetric water content at freezeback divided by porosity, influences runoff as soils with greater pore space filled with frozen water restrict infiltration and promotes runoff. In fall 2017, soils froze in late October at a relatively low moisture content in the near surface profile ( $VWC < 5\%$  and  $S_i = 0.20$ ). This moisture content was the lowest of any years observed, yet pre-freezeback values as high as 0.5 occurred in some years. As with soil temperature,  $S_i$  was varied within the range of the observed six-year record for the 2018 winter case. Runoff increased approximately linearly with increasing  $S_i$ , and results indicate that within the range of observation, pre-freezeback soil moisture can more than triple the expected runoff for a given year (Table 3). For every 5% increase in  $S_i$  from 0.2, runoff increased ~12 mm with slightly greater increases when dry. It is important to note that 2018 was a high snow year with low initial  $S_i$ .

Zhao and Gray (1999) use temperature within the top 40 cm at the onset of melt along with a nighttime refreezing parameter to establish the influence of soil thermal status on infiltration. The initial soil temperature (top 40 cm) during 2018 was  $-2\text{ }^\circ\text{C}$ , which was used to run all climate change scenarios in Section 4.3.1. However, between 2013 and 2018 soil temperatures at the onset of melt were as low as  $-8\text{ }^\circ\text{C}$  within the top 40 cm, which reflected cold years with limited snow. The 2018 winter simulation was run with temperatures from  $-0.5\text{ }^\circ\text{C}$  to  $-8\text{ }^\circ\text{C}$ , and results indicate a strong influence of temperature on runoff generation (Table 3). Runoff generation was zero at temperatures warmer than  $-1.5\text{ }^\circ\text{C}$  and increased in a negative exponential manner with declining temperatures and at  $-8\text{ }^\circ\text{C}$ , 94 mm of runoff was simulated compared with 34 mm as the base case.

#### 4.3.2 Climate Change Scenarios

To test the accuracy of CRHM against observed data, simulations were set up under current climate conditions (T0-P1) for snowpack SWE from 2013-2018 (Figure 6a) and surface runoff during the 2017-2018 winter (Figure 6b). Surface runoff data only exists for 2017-2018 as the runoff collectors were installed in March 2018. In general, CRHM's simulations overestimated peak snowpack SWE, total surface runoff and underestimated mid-winter melt events (Figure 6). Annual peak simulated SWE was higher by an average of ~30 mm over simulated years, but the timing of snow accumulation and the start/end of the snow season is consistent with the observed data (Figure 6a) and over all simulated years matched the observed data within 10 days. Simulated surface runoff did not match observed runoff in terms of timing as simulated runoff occurs at the very end of the snow season while observed runoff had two distinct melt periods (Figure 6b). While total observed runoff (15 and 23 mm) was less than simulated runoff (34 mm), snowmelt partitioning between infiltration and runoff were similar based on the calculated runoff ratios of 0.3 and 0.2, respectively. Observed and simulated total runoff may differ between because by the time the runoff collectors were installed, some of the snowpack had already melted, yielding a smaller total runoff. Additionally, CRHM underestimates the magnitude and duration of mid-winter melt events in all simulated years. For example, CRHM simulated an 8 mm melt event over five days in 2018 compared to observed where the mid-winter melt event caused snowpack SWE to decrease by 83, 45 and 51 mm, respectively for stations 1, 2 and 3 over ~12 days. It is unclear as to why this underestimation occurred, although it may be due to different locations between the SWE sensors and the meteorological data used to drive the model. Note that CRHM was not calibrated but driven by observation data and measured soil parameters (Table 1 and 2).

Modelled increases in temperature without an alteration in precipitation resulted in an expected reduction

in simulated SWE, a shorter snow season and longer and larger mid-winter melt events (Figure 7a). Over the simulated years in scenarios T2-P1, T4-P1 and T6-P1, peak snowpack SWE decreased by an average of 21, 35 and 42 %, respectively (Table 4), where deviation from current conditions (T0-P1) was amplified in winters with a higher peak SWE (Figure 7a). Duration of the snow season decreased by averages of 10, 37 and 61 days, respectively, some of which were the result of mid-winter melt that eliminated the entire snowpack by January or February in low snow years (i.e. 2013-2014, Figure 7a). The presence of mid-winter melt events is an emergent process with warming as its timing moves successively earlier into the winter season. Under these warming scenarios, average mid-winter melt duration increased from 5 days under T0-P1 to 7, 14 and 11 days, respectively for scenarios T2-P1, T4-P1 and T6-P1, respectively. Average snowmelt volume during the mid-winter melt also increased from 12 mm under T0-P1 to 26, 39 and 43 mm, respectively, all of which infiltrated into the frozen ground. Spring snowmelt runoff was small for all warming-only scenarios and decreased from a 5-year average of 11 mm under current conditions to 8, 1 and 0 mm, respectively for each of the two-degree temperature increases (Figure 8a) which decrease the average runoff ratio from 0.38 to 0.1, 0.01 and 0, respectively (Table 4).

Simulated increases in daily precipitation without changes in temperature increased peak SWE all years by averages of 12, 28 and 36 % in scenarios T0-P1.15, T0-P1.2 and T0-P1.3, respectively compared to initial conditions (Figure 7b). Snow season duration is similar to initial conditions and only increased by an average of 7, 8 and 8 days, respectively among precipitation scenarios. Unlike the temperature scenarios, there are no distinct mid-winter melt events among years and snowpack SWE continues to increase until the spring snowmelt event. Surface runoff of spring snowmelt increased from the 11 mm average for current conditions greater daily precipitation, and averaged 20, 25 and 29 mm, respectively (Figure 8b) which kept runoff ratios similar to current conditions (0.2) and averaged 0.17, 0.18 and 0.21, respectively (Table 4).

An increase of both temperature and precipitation slightly lessened the effect of climate change on snowpack SWE while surface runoff exhibited the most variability among all climate scenarios. Peak SWE and snow duration under T2-P1.2 are similar to initial conditions but decrease considerably with continued warming with T4-P1.2 and T6-P1.2 (Figure 7c). Average peak snowpack SWE and snow season duration both decreased by an average of 0.2, 24 and 32 %, respectively and by an average of 1, 17 and 61 days, respectively in scenarios T2-P1.2, T4-P1.2 and T6-P1.2 (Table 4). Mid-winter melt events become increasingly prominent with warming and mid-melt duration increased to 6, 12 and 14 days from 5 days under T0-P1. Mid-winter melt volumes also increased under these conditions to 19, 40 and 44 mm, respectively from 5 mm under T0-P1. Surface runoff from end of season snowmelt increased initially in scenario T2-P1.2 to 20 mm from 11 mm in T0-P1, but then decreased to 10 and 3 mm in scenarios T4-P1.2 and T6-P1.2, respectively (Figure 8c). Runoff ratios were maintained at T2-P1.2 and averaged 0.21 but decreased with continued warming to 0.16 and 0.03, respectively indicating that more meltwater infiltrates under warmer scenarios. A summary of the CRHM simulations are in Table 4 but detailed results from the climate change simulations can be found in Table A1.

## 5. DISCUSSION

At present, two watersheds in the AOSR inform much of our understanding of hydrology (Ketcheson et al., 2017; Nicholls et al., 2016; Spennato, Ketcheson, Mendoza, & Carey, 2018), carbon dynamics (Clark et al., 2019; Clark, Humphreys, & Carey, 2020) and water quality (Biagi et al., 2019; Kessel et al., 2018; Simhayov et al., 2017) for integrated constructed ecosystems. With only two examples over a relatively short time period, it is uncertain as to how representative these systems are and whether early findings can be used to evaluate performance and help guide future design. While ecosystems are built for long-term sustainability, they are dynamic and rapidly changing and it is expected that their hydrological behaviour will evolve in response to changes in vegetation, soil properties, water quality and climate. Examination of winter

processes in constructed ecosystems is scarce (Kelln et al., 2009; Ketcheson & Price, 2016b; Meier & Barbour, 2002), despite five months of temperatures below freezing. In this work we used detailed field observations combined with a purpose-built hydrological model to better understand how ecosystem properties and a changing climate influence hydrological fluxes.

### 5.1 *What controls patterns of snow accumulation and melt on SFW?*

The greatest SWE variability arose from differences in slope position on the hummocks (Figure 3), where snow accumulated at the bottoms of the hillslopes and decreased towards the crest. The base of hillslope accumulates blowing snow from the relatively flat wetlands and uplands, whereas the crest of the hummocks are exposed to wind erosion as well as enhanced sublimation (Pomeroy & Essery, 1999). SWE distribution among aspects showed no significant difference ( $p > 0.05$ ), as wind direction was variable throughout the winter (data not shown). SWE decline was similar between the wetland and upland areas (Figure 4a and b) as both have a relatively flat terrain and receive similar amounts of solar radiation throughout the day. Melt was most variable on the hummocks as slope aspects are exposed to different irradiances and south-facing slopes melted earlier and faster than north-facing slopes (Figure 4).

Vegetation often exerts a strong control on snow accumulation and melt patterns as blowing snow from surrounding landscapes are trapped by shrubs and trees plus snow interception on their canopies (Boon, 2012; Pomeroy et al., 2006, 1998). However, due to the relatively young age of the SFW, topography was the dominant control on snow accumulation and melt as the vegetation is in the early stages of development and has similar height and density across landscape units, despite species differences. This is common among more recently reclaimed ecosystems (Ketcheson & Price, 2016b) which are considerably younger than their natural analogues and require decades for their vegetation to develop fully. As vegetation emerges, increased roughness will lower the influence of wind on scouring and enhance snow trapping via decreased turbulence. However, direct interception may lower snow accumulation due to enhanced sublimation. From a melt perspective, vegetation reduces shortwave radiation to the surface yet enhances long-wave fluxes to the snowpack, thus altering the snowmelt radiative regime (Pomeroy et al., 2009). While aspect plays an important role on how vegetation influences melt (Ellis & Pomeroy, 2007; Ellis, Pomeroy, Essery, & Link, 2011), as the canopy closes melt will be delayed further into spring (Dickerson-Lange et al., 2017). This influence can be observed by comparing SFW with other nearby reclamation landscapes in more advanced stages of regrowth (Figure 9). Two mature reclaimed forests, South Bison Hill (~20-year-old mature aspen/white spruce stand) and Jack Pine (~30-year-old jack pine stand) have delayed melt compared with the newly reclaimed Coke Beach site (~10-year young aspen) and the SFW (~6 years). Both sites with tall vegetation had deeper snowpacks that persisted later into April and were less susceptible to early melt. However, the actual snow-free dates were remarkably similar.

### 5.2 *The importance of hillslopes on snowmelt runoff generation*

The snowmelt period is a critical input of freshwater available to WBP ecosystems, including constructed systems, which rely heavily on this input to replace storage deficits for the upcoming growing season as well as persist in a climate with a long-term water deficit (Devito et al., 2012). Snowmelt also offers an important input of freshwater to dilute the elevated salinity and sodium concentrations that are ubiquitous within the reclaimed landscape (Biagi et al., 2019; Kessel et al., 2018). Reconstructed landscapes need to balance between optimizing soil storage for vegetation productivity while providing sufficient water to surrounding landscapes. The hillslope hummocks in the SFW were initially designed to provide groundwater to the adjacent lowlands via recharge and were not expected to produce much surface runoff. The hummocks have no confining soil layer at depth and most of its meltwater infiltrates and percolates downwards. Groundwater flow is the primary delivery of water to the lowlands (Lukenbach et al., 2019), whereas surface runoff is limited to snowmelt periods and potentially extreme rain events.

While total surface snowmelt runoff was similar on both south and north-facing slopes (15 mm and 23 mm, respectively), their timing and rates differed where south-facing slopes melted much earlier and faster (Figure 5). The increased air temperature and radiation in mid-March induced melt-generated runoff on the south-facing slope, yet north-facing slope melt was delayed and no runoff occurred until mid-April when conditions remained warm and a rapid decline in snowpacks were observed (Figure 5). The SFW hummocks are constructed from Pf sand and tailings sand materials which have average hydraulic conductivities of  $1.1 \times 10^{-4}$  m/s and  $6.7 \times 10^{-4}$  m/s and an average unfrozen infiltration capacity of  $1.8 \times 10^{-4}$  m/s (Table 1). These hummocks remain unsaturated all year as water infiltrates and percolates downwards to recharge groundwater at depth (Lukenbach et al., 2019), which can result in low antecedent moisture contents (VWC <5 % on Nov 1, data not shown) prior to freeze-up throughout the upper soil column. However, this varied over the five years of observation. In 2018, these soils maintain a relatively high infiltration capacity when frozen and exceed the maximum melt rate on both the north and south-facing slopes ( $5.8 \times 10^{-7}$  and  $3.7 \times 10^{-7}$  m/s, respectively) therefore partitioning most of the snowmelt water as infiltration. Surface runoff ratios at SFW (~0.3) were much less than those reported by Ketcheson and Price (2016) (0.7-0.9). The hillslopes on Nikanotee fen by comparison, have finer soil textures, considerably higher moisture content overall, and low surface infiltration capacities (Ketcheson & Price, 2016a), resulting in much higher surface runoff during spring snowmelt (Ketcheson & Price, 2016b).

Using CRHM, a well-established platform for simulating winter hydrological processes, the influence of soil properties on the partitioning of meltwater was evaluated. Soil texture alone had only a modest influence, increasing runoff as texture became finer. However, this is complicated by differences in antecedent moisture that would typically accompany finer textures. As antecedent soil wetness increased, melt generated runoff increased as snowmelt infiltration became more restricted (Table 3). Progressively finer textures will increase runoff, an important implication for landscape design and an observation which reconciles results presented here and those of Ketcheson and Price (2016a). Surprisingly, soil temperature at the onset of melt had a large influence on limiting infiltration. In 2018, soils were relatively warm (-2 °C) under a deep snowpack, and simulations suggest that if soils were colder, considerably more runoff would have been generated (Table 3). However, a negative feedback exists as deeper snowpacks that can generate more runoff insulate soils (enhancing infiltration), whereas thin snowpacks with less potential for runoff generation would have colder soils, enhancing runoff. While texture can be used to directly enhance or reduce melt runoff, a subtle relationship exists that provides for a large range of runoff ratios based on the combination of SWE and soil temperature. From an operational perspective, upland hillslopes can be designed using textural classes to either enhance or limit direct runoff from hillslopes to provision lowland and wetland systems with water. However, model results suggest a large range of variability driven by moisture content and temperature, even within coarse textured soils that were expected to produce little snowmelt runoff. As vegetation on uplands grows, snow accumulation may slightly increase, and melt will be delayed. Furthermore, vegetation will increase soil macro-porosity and infiltration capacity, reducing runoff potential.

### *5.3 What is the influence of climate change on winter processes?*

While the WBP is expected to be warmer and wetter with the influence of climate change, an increase in evapotranspiration could lead to an overall drier environment (Ireson et al., 2015; Thompson, Mendoza, & Devito, 2017). CRHM simulations for winter indicate a decrease in snow season length, runoff, peak SWE and an increase in the presence and magnitude of mid-winter melt events. While it suggests that the increase in precipitation by a factor of 1.2 offsets the increase in temperature by 2 °C, further warming clearly decreases the snowpack SWE and shortens the snow season and therefore more of the annual precipitation is delivered as rain instead of snow. Mid-winter melt events are increasingly prevalent under warming scenarios and are expected to become more common in reconstructed systems and may result in the complete loss of the snowpack in drier years when the snowpack is small. Surface runoff is expected to decrease considerably

with increased warming and may cease under the warmest scenarios. However, the role of potentially colder runoff-enhancing soils with decreasing snowpacks was not captured in the model. With a smaller snowpack, less meltwater is partitioned as runoff, which may increase soil and groundwater recharge. The influence of climate change may be underestimated by CRHM, as results indicate that simulations overestimate SWE and to a lesser extent runoff compared to observed data. As a result, actual snowpack SWE, runoff and mid-winter melt events with the onset of climate change could be enhanced compared to simulated results in this study. While an increase in precipitation (delivered as rain) may offset the effects of a lengthened growing season and increase in evapotranspiration, it is expected that the water balance of these systems will be impacted over time. The influence of climate change on SFW combined with expected changes in vegetation and soil development provide considerable uncertainty as to how the rate, timing and magnitude of hydrological fluxes within the landscape will change. With the potential for these systems to become increasingly drier with the onset of climate change, it is critical that future design of these constructed systems maximize water retention and storage such as increasing hummock recharge (Ketcheson et al., 2017; Lukenbach et al., 2019) and maintaining high infiltration capacity-soils to enhance groundwater recharge.

## CONCLUSIONS

The future expansion of bitumen extraction via surface mining projected for the coming decades will result in thousands of hectares of land that will need to be reclaimed. A better understanding of the evolution of runoff pathways and surface-groundwater interactions are required to assess their trajectory and long-term sustainability, which will influence water management and future design of these systems. Results presented here highlight that topography currently controls snow distribution and melt, as vegetation has little influence on winter processes during these early stages. Surface runoff from hillslopes in a large snow year was higher than expected (up to 30 %) and offers a potentially important transport mechanism of water towards the wetland that can help replenish water deficits as well as offer a supply of fresh water to a relatively saline wetland. The remainder of meltwater infiltrated into the unsaturated frozen soils and was partitioned between the rooting zone and deeper percolation. This study provides an important contrast to the other constructed wetland-upland system in the AOSR where the majority of meltwater was transported to the lowland via surface runoff which highlights the influence of construction design and practice on the system's hydrology. The Cold Regions Hydrological Model simulations of snowmelt partitioning with varying soil conditions indicate that antecedent soil saturation (VWC/porosity) and soil temperature had the greatest influence on partitioning snowmelt as surface runoff, while soil texture alone had a moderate affect. Observed and modelled surface runoff results within the AOSR provide evidence that partitioning between surface runoff and infiltration can somewhat be controlled by hillslope construction materials when designed these reclaimed systems. Under various scenarios of a warmer and wetter climate, the Cold Regions Hydrological Model predicts that average annual peak SWE and duration of the snow season could decline by up to 52 % and up to 61 days, respectively while snowmelt runoff ceases completely under the warmest scenarios. This may lead to drier conditions with the onset of climate change as water deficits could increase each year as an increasingly smaller snowpack cannot replenish water stores.

## ACKNOWLEDGEMENTS

We thank two anonymous reviewers for their contributions in improving this paper. We would also like to thank Dr. M. Graham Clark for detailed comments, help with figures, and suggestions to the manuscript. Funding for this research was provided by Syncrude Canada Ltd. and Global Water Futures. We would like to thank all field work assistance including Keegan Smith, Ian Martin, M. Graham Clark, Dr. Michael Treberg and Dr. Gordon Drewitt. We also acknowledge Angus MacDonald (McMaster University) for help with CRHM setup, Sean Leipe (McMaster University) for help with the LiDAR data and ArcGIS and O'Kane Consultants for assistance with meteorological data.

## Data Availability Statement

The data that support the findings of this study are available from the corresponding authors upon reasonable

request.

## References

- Ayers, H. D. (1959). Influence of soil profile and vegetation characteristics on net rainfall supply to runoff. *Proceedings of Hydrology Symposium, 1*, 198–205.
- Biagi, K. M., Oswald, C. J., Nicholls, E. M., & Carey, S. K. (2019). Increases in salinity following a shift in hydrologic regime in a constructed wetland watershed in a post-mining oil sands landscape. *Science of the Total Environment, 653*, 1445–1457. <https://doi.org/10.1016/j.scitotenv.2018.10.341>
- Boon, S. (2012). Snow accumulation following forest disturbance. *Ecohydrology, 5*, 279–285. <https://doi.org/10.1002/eco.212>
- Canada’s Oil & Natural Gas Producers. (2017). *Introduction to Oil Sands*. <https://doi.org/10.1346/cms-wls-22>
- Carrera-Hernandez, J. J., Smerdon, B. D., & Mendoza, C. A. (2012). Estimating groundwater recharge through unsaturated flow modelling: Sensitivity to boundary conditions and vertical discretization. *Journal of Hydrology, 452–453*, 90–101. <https://doi.org/10.1016/j.jhydrol.2012.05.039>
- Clark, M. G., Humphreys, E., & Carey, S. K. (2019). The initial three years of carbon dioxide exchange between the atmosphere and a reclaimed oil sand wetland. *Ecological Engineering, 135*, 116–126. <https://doi.org/10.1016/j.ecoleng.2019.05.016>
- Clark, M. G., Humphreys, E. R., & Carey, S. K. (2020). Low methane emissions from a boreal wetland constructed on oil sand mine tailings. *Biogeosciences Discussions, 17*, 667–682. <https://doi.org/10.5194/bg-2019-271>
- Cordeiro, M. R. C., Wilson, H. F., Vanrobaeys, J., Pomeroy, J. W., & Fang, X. (2017). Simulating cold-region hydrology in an intensively drained agricultural watershed in Manitoba, Canada, using the Cold Regions Hydrological Model. *Hydrology and Earth System Sciences, 21*, 3483–3506.
- Daly, C., Price, J., Rezanezhad, F., Pouliot, R., Rochefort, L., & Graf, M. D. (2012). Initiatives in oil sand reclamation: Considerations for building a fen peatland in a post-mined oil sands landscape. In D. H. Vitt & J. Bhatti (Eds.), *Restoration and Reclamation of Boreal Ecosystems: Attaining Sustainable Development* (pp. 179–198). Cambridge University Press.
- Devito, K. J., Creed, I. F., & Fraser, C. J. D. (2005). Controls on runoff from a partially harvested aspen-forested headwater catchment, Boreal Plain, Canada. *Hydrological Processes, 19*(1), 3–25. <https://doi.org/10.1002/hyp.5776>
- Devito, K. J., Hokanson, K. J., Moore, P. A., Kettridge, N., Anderson, A. E., Chasmer, L., . . . Waddington, J. M. (2017). Landscape controls on long-term runoff in subhumid heterogeneous Boreal Plains catchments. *Hydrological Processes, 31*(15), 2737–2751. <https://doi.org/10.1002/hyp.11213>
- Devito, K. J., Mendoza, C., & Qualizza, C. (2012). *Conceptualizing water movement in the Boreal Plains: Implications for watershed reconstruction*. Synthesis report prepared for the Canadian Oil Sands Network for Research and Development, Environmental and Reclamation Research Group.
- Dickerson-Lange, S. E., Gersonde, R. F., Hubbart, J. A., Link, T. E., Nolin, A. W., Perry, G. H., . . . Lundquist, J. D. (2017). Snow disappearance timing is dominated by forest effects on snow accumulation in warm winter climates of the Pacific Northwest, United States. *Hydrological Processes, 31*(10), 1846–1862. <https://doi.org/10.1002/hyp.11144>
- Dobchuk, B. S., Shurniak, R. E., Barbour, S. L., Kane, M. A. O., & Song, Q. (2013). Long-term monitoring and modelling of a reclaimed watershed cover on oil sands tailings. *International Journal of Mining, Reclamation and Environment, 27*(3), 180–210. <https://doi.org/10.1080/17480930.2012.679477>

- Ellis, C. R., & Pomeroy, J. W. (2007). Estimating sub-canopy shortwave irradiance to melting snow on forested slopes. *Hydrological Processes*, *21*(19), 2581–2593. <https://doi.org/10.1002/hyp>
- Ellis, C. R., Pomeroy, J. W., Brown, T., & MacDonald, J. (2010). Simulation of snow accumulation and melt in needleleaf forest environments. *Hydrology and Earth System Sciences*, *14*(6), 925–940. <https://doi.org/10.5194/hess-14-925-2010>
- Ellis, C. R., Pomeroy, J. W., Essery, R. L. H., & Link, T. E. (2011). Effects of needleleaf forest cover on radiation and snowmelt dynamics in the Canadian Rocky Mountains. *Canadian Journal of Forest Research*, *41*(3), 608–620. <https://doi.org/10.1139/X10-227>
- Elshorbagy, A., Jutla, A., Barbour, L., & Kells, J. (2005). System dynamics approach to assess the sustainability of reclamation of disturbed watersheds. *Canadian Journal of Civil Engineering*, *32*, 144–158. <https://doi.org/10.1139/104-112>
- Elshorbagy, A., Jutla, A., & Kells, J. (2007). Simulation of the hydrological processes on reconstructed watersheds using system dynamics. *Hydrological Sciences*, *52*(3), 538–562.
- Environment Canada. (2019). Canadian Climate Normals 1981-2010 Station Data. Retrieved December 1, 2019, from [https://climate.weather.gc.ca/climate\\_normals/results-e.html?stnID=2519&dispBack=0&month1=0&month2=12#legenda](https://climate.weather.gc.ca/climate_normals/results-e.html?stnID=2519&dispBack=0&month1=0&month2=12#legenda)
- Fang, X., & Pomeroy, J. W. (2007). Snowmelt runoff sensitivity analysis to drought on the Canadian prairies. *Journal of Glaciology*, *21*, 2594–2609. <https://doi.org/10.1002/hyp>
- Fang, X., & Pomeroy, J. W. (2010). Modelling blowing snow redistribution to prairie wetlands. *Hydrological Processes*, *23*, 2557–2569. <https://doi.org/10.1002/hyp>
- Fang, X., Pomeroy, J. W., Ellis, C. R., MacDonald, M. K., DeBeer, C. M., & Brown, T. (2013). Multi-variable evaluation of hydrological model predictions for a headwater basin in the Canadian Rocky Mountains. *Hydrology and Earth System Sciences*, *17*(4), 1635–1659. <https://doi.org/10.5194/hess-17-1635-2013>
- Fang, X., Pomeroy, J. W., Westbrook, C. J., Guo, X., Minke, A. G., & Brown, T. (2010). Prediction of snowmelt derived streamflow in a wetland dominated prairie basin. *Hydrology and Earth System Sciences*, *14*(6), 991–1006. <https://doi.org/10.5194/hess-14-991-2010>
- Ferone, J. M., & Devito, K. J. (2004). Shallow groundwater-surface water interactions in pond-peatland complexes along a Boreal Plains topographic gradient. *Journal of Hydrology*, *292*, 75–95. <https://doi.org/10.1016/j.jhydrol.2003.12.032>
- Freeze, R. A., & Cherry, J. A. (1979). Groundwater Resource Extraction. In *GroundWater* (p. 337). Englewood Cliffs: Prentice Hall.
- Garnier, B. J., & Ohmura, A. (1970). The evaluation of surface variations in solar radiation income. *Journal of Applied Meteorology*, *13*(1), 21–34.
- Hilbert, D. W., Roulet, N., & Moore, T. (2000). Modelling and analysis of peatlands as dynamical systems. *Journal of Ecology*, *88*(2), 230–242. <https://doi.org/10.1046/j.1365-2745.2000.00438.x>
- Huang, M., Barbour, S. L., & Carey, S. K. (2015). The impact of reclamation cover depth on the performance of reclaimed shale overburden at an oil sands mine in Northern Alberta, Canada. *Hydrological Processes*, *29*, 2840–2854. <https://doi.org/10.1002/hyp.10229>
- Huang, M., Hilderman, J. N., & Barbour, L. (2015). Transport of stable isotopes of water and sulphate within reclaimed oil sands saline-sodic mine overburden. *Journal of Hydrology*, *529*, 1550–1561. <https://doi.org/10.1016/j.jhydrol.2015.08.028>
- Ireson, A. M., Barr, A. G., Johnstone, J. F., Mamet, S. D., van der Kamp, G., Whitfield, C. J., ... Sagin, J. (2015). The changing water cycle: the Boreal Plains ecozone of Western Canada. *Wiley Interdisciplinary*

- Reviews: Water*, 2(5), 505–521. <https://doi.org/10.1002/wat2.1098>
- Kelln, C., Barbour, L., & Qualizza, C. (2007). Preferential Flow in a Reclamation Cover: Hydrological and Geochemical Response. *Journal of Geotechnical and Geoenvironmental Engineering*, 133(10), 1277–1289. [https://doi.org/10.1061/\(ASCE\)1090-0241\(2007\)133:10\(1277\)](https://doi.org/10.1061/(ASCE)1090-0241(2007)133:10(1277))
- Kelln, C., Barbour, S. L., & Qualizza, C. (2008). Controls on the spatial distribution of soil moisture and solute transport in a sloping reclamation cover. *Canadian Geotechnical Journal*, 45, 351–366. <https://doi.org/10.1139/T07-099>
- Kelln, C., Barbour, S. L., & Qualizza, C. (2009). Fracture-Dominated Subsurface Flow and Transport in a Sloping Reclamation Cover. *Vadose Zone Journal*, 8(1), 96. <https://doi.org/10.2136/vzj2008.0064>
- Keshta, N., Elshorbagy, A., & Carey, S. K. (2009). A generic system dynamics model for simulating and evaluating the hydrological performance of reconstructed watersheds. *Hydrology and Earth System Sciences Discussions*, 13, 865–881. <https://doi.org/10.5194/hessd-5-1441-2008>
- Kessel, E. D., Ketcheson, S. J., & Price, J. S. (2018). The distribution and migration of sodium from a reclaimed upland to a constructed fen peatland in a post-mined oil sands landscape. *Science of the Total Environment*, 630, 1553–1564. <https://doi.org/10.1016/j.scitotenv.2018.02.253>
- Kessler, S., Barbour, S. L., van Rees, K. C. J., & Dobchuk, B. S. (2010). Salinization of soil over saline-sodic overburden from the oil sands in Alberta. *Canadian Journal of Soil Science*, 90, 637–647. <https://doi.org/10.4141/cjss10019>
- Ketcheson, S. J., & Price, J. S. (2016a). A comparison of the hydrological role of two reclaimed slopes of different age in the Athabasca Oil Sands Region, Alberta, Canada. *Canadian Geotechnical Journal*, 53(June), 1533–1546. <https://doi.org/10.1139/cgj-2015-0391>
- Ketcheson, S. J., & Price, J. S. (2016b). Snow hydrology of a constructed watershed in the Athabasca oil sands region, Alberta, Canada. *Hydrological Processes*, 30(14), 2546–2561. <https://doi.org/10.1002/hyp.10813>
- Ketcheson, S. J., Price, J. S., Carey, S. K., Petrone, R. M., Mendoza, C. A., & Devito, K. J. (2016). Constructing fen peatlands in post-mining oil sands landscapes: Challenges and opportunities from a hydrological perspective. *Earth-Science Reviews*, 161, 130–139. <https://doi.org/10.1016/j.earscirev.2016.08.007>
- Ketcheson, S. J., Price, J. S., Sutton, O., Sutherland, G., Kessel, E. D., & Petrone, R. M. (2017). The hydrological functioning of a constructed fen wetland watershed. *Science of the Total Environment*, 603–604, 593–605. <https://doi.org/10.1016/j.scitotenv.2017.06.101>
- Knox, S. H., Carey, S. K., & Humphreys, E. R. (2012). Snow surface energy exchanges and snowmelt in a shrub-covered bog in eastern Ontario, Canada. *Hydrological Processes*, 26(12), 1877–1891. <https://doi.org/10.1002/hyp.9289>
- Krogh, S. A., & Pomeroy, J. W. (2018). Recent changes to the hydrological cycle of an Arctic basin at the tundra-taiga transition. *Hydrology and Earth System Sciences*, 22(7), 3993–4014. <https://doi.org/10.5194/hess-22-3993-2018>
- Lukenbach, M. C., Spencer, C. J., Mendoza, C. A., Devito, K. J., Landhausser, S. M., & Carey, S. K. (2019). Evaluating How Landform Design and Soil Covers Influence Groundwater Recharge in a Reclaimed Watershed. *Water Resources Research*, 55(8), 6464–6481. <https://doi.org/10.1029/2018WR024298>
- Marks, D., Domingo, J., Susong, D., Link, T., & Garen, D. (1999). A spatially distributed energy balance snowmelt model for application in mountain basins. *Hydrological Processes*, 13, 1935–1959.
- Meehl, G. A., Stocker, T. F., Collins, W. D., Friedlingstein, P., Gaye, A. T., Gregory, J. M., ... Zhao, Z.-C. (2007). Global Climate Projections. In S. Solomon, D. Qin, M. Manning, Z. Chen, M. Marquis,

- K. B. Averyt, ... H. L. Miller (Eds.), *Climate Change 2007 - The Physical Science Basis. Contribution of Working Group I to the Fourth Assessment Report of the Intergovernmental Panel on Climate Change*. (pp. 747–845). Cambridge, United Kingdom and New York, NY, USA: Cambridge University Press. <https://doi.org/10.1109/ICEPT.2010.5582830>
- Meier, D. E., & Barbour, S. L. (2002). *Monitoring of Cover and Watershed Performance for Soil Covers Placed Over Saline-Sodic Shale Overburden From Oilsands Mining*. *Journal American Society of Mining and Reclamation*. <https://doi.org/10.21000/jasmr02010602>
- Nicholls, E. M., Carey, S. K., Humphreys, E. R., Clark, M. G., & Drewitt, G. B. (2016). Multi-year water balance assessment of a newly constructed wetland, Fort McMurray, Alberta. *Hydrological Processes*, *30*, 2739–2753. <https://doi.org/10.1002/hyp.10881>
- NorthWind Land Resources Inc. (2012). *Sandhill Fen Baseline Soil Sampling - Syncrude Canada Ltd.*
- Nwaishi, F., Petrone, R. M., Price, J. S., Ketcheson, S., Slawson, R., & Andersen, R. (2015). Impacts of donor-peat management practices on the functional characteristics of a constructed fen. *Ecological Engineering*, *81*, 471–480. <https://doi.org/10.1016/j.ecoleng.2015.04.038>
- OSWWG. (2008). *Guideline for wetland establishment on reclaimed oil sands leases (2nd edition)*. Alberta Environment. Fort McMurray, Alberta: Prepared by Harris, M.L. of Lorax Environmental for the Wetlands and Aquatics Subgroup of the Reclamation Working Group of the Cumulative Environmental Management Association. Retrieved from <http://environment.gov.ab.ca/info/library/6854.pdf>
- Pomeroy, J. W., Bewley, D. S., Essery, R. L. H., Hedstrom, N. R., Link, T., Granger, R. J., ... Janowicz, J. R. (2006). Shrub tundra snowmelt. *Hydrological Processes*, *20*, 923–941. <https://doi.org/10.1002/hyp.6124>
- Pomeroy, J. W., & Essery, R. L. H. (1999). Turbulent fluxes during blowing snow: Field tests of model sublimation predictions. *Hydrological Processes*, *13*(18), 2963–2975.
- Pomeroy, J. W., Fang, X., & Ellis, C. (2012). Sensitivity of snowmelt hydrology in Marmot Creek, Alberta, to forest cover disturbance. *Hydrological Processes*, *26*(12), 1891–1904. <https://doi.org/10.1002/hyp.9248>
- Pomeroy, J. W., Gray, D. M., Brown, T., Hedstrom, N. R., Quinton, W. L., Granger, R. J., & Carey, S. K. (2007). The cold regions hydrological model: a platform for basing process representation and model structure on physical evidence. *Hydrological Processes*, *21*, 2650–2667. <https://doi.org/10.1002/hyp>
- Pomeroy, J. W., Gray, D. M., Shook, K. R., Toth, B., Essery, R. L. H., Pietroniro, A., & Hedstrom, N. (1998). An evaluation of snow accumulation and ablation processes for land surface modelling. *Hydrological Processes*, *12*, 2339–2367.
- Pomeroy, J. W., Marks, D., Link, T., Ellis, C. R., Hardy, J., Rowlands, A., & Granger, R. J. (2009). The impact of coniferous forest temperature on incoming longwave radiation to melting snow. *Hydrological Processes*, *23*(17), 2513–2525. <https://doi.org/10.1002/hyp>
- Price, J. S. (1987). Influence of wetland and mineral terrain types on snowmelt runoff in the subarctic. *Canadian Water Resources Journal*, *12*(2). <https://doi.org/10.4296/cwrj1202043>
- Price, J. S., & Fitzgibbon, J. E. (1987). Groundwater storage - streamflow relations during winter in a subarctic wetland, Saskatchewan. *Canadian Journal of Earth Sciences*, *24*, 2074–2081.
- Price, J. S., McLaren, R. G., & Rudolph, D. L. (2010). Landscape restoration after oil sands mining: conceptual design and hydrological modelling for fen reconstruction. *International Journal of Mining, Reclamation and Environment*, *24*(2), 109–123. <https://doi.org/10.1080/17480930902955724>
- Quinton, W. L., & Baltzer, J. L. (2013). The active-layer hydrology of a peat plateau with thawing permafrost (Scotty Creek, Canada). *Hydrogeology Journal*, *21*(1), 201–220. <https://doi.org/10.1007/s10040-012-0935-2>

- Quinton, W. L., Bemrose, R. K., Zhang, Y., & Carey, S. K. (2009). The influence of spatial variability in snowmelt and active layer thaw on hillslope drainage for an alpine tundra hillslope. *Hydrological Processes*. <https://doi.org/10.1002/hyp.7327>
- Quinton, W. L., Carey, S. K., & Goeller, N. T. (2004). Snowmelt runoff from northern alpine tundra hillslopes: major processes and methods of simulation. *Hydrology and Earth System Sciences*, 8(5), 877–890. <https://doi.org/10.5194/hess-8-877-2004>
- R Core Team. (2018). A Language and Environment for Statistical Computing. R Foundation for Statistical Computing, Vienna Austria (URL). Vienna, Austria. Retrieved from <https://www.r-project.org/>
- Rasouli, K., Pomeroy, J. W., Janowicz, J. R., Carey, S. K., & Williams, T. J. (2014). Hydrological sensitivity of a northern mountain basin to climate change. *Hydrological Processes*, 28, 4191–4208. <https://doi.org/10.1002/hyp.10244>
- Rasouli, K., Pomeroy, J. W., & Whitfield, P. H. (2019). Are the effects of vegetation and soil changes as important as climate change impacts on hydrological processes? *Hydrology and Earth System Sciences*, 23(12), 4933–4954. <https://doi.org/10.5194/hess-23-4933-2019>
- Redding, T., & Devito, K. (2011). Aspect and soil textural controls on snowmelt runoff on forested Boreal Plain hillslopes. *Hydrology Research*, 42(4), 250–267. <https://doi.org/10.2166/nh.2011.162>
- Rooney, R. C., Bayley, S. E., & Schindler, D. W. (2012). Oil sands mining and reclamation cause massive loss of peatland and stored carbon. *Proceedings of the National Academy of Sciences of the United States of America*, 109(13), 4933–4937. <https://doi.org/10.1073/pnas.1117693108>
- Rouse, W. R. (2000). The energy and water balance of high-latitude wetlands: controls and extrapolation. *Global Change Biology*, 6(Suppl. 1), 59–68. <https://doi.org/10.1046/j.1365-2486.2000.06013.x>
- Shook, K., Pomeroy, J. W., Spence, C., & Boychuk, L. (2013). Storage dynamics simulations in prairie wetland hydrology models: evaluation and parameterization. *Hydrological Processes*, 27(13), 1875–1889. <https://doi.org/10.1002/hyp.9867>
- Shurniak, R. E., & Barbour, S. L. (2002). Modeling of Water Movement Within Reclamation Covers on Oilsands Mining Overburden Piles. In *Proceedings of the National Meeting of the American Society of Mining and Reclamation* (pp. 622–644). Lexington, Ky.: American Society of Mining and Reclamation (ASMR). <https://doi.org/10.21000/JASMR02010622>
- Sicart, J. E., Pomeroy, J. W., Essery, R. L. H., & Bewley, D. (2006). Incoming longwave radiation to melting snow: observations, sensitivity and estimation in northern environments. *Hydrological Processes*, 20, 3697–3708. <https://doi.org/10.1002/hyp>
- Simhayov, R. B., Price, J. S., Smeaton, C. M., Parsons, C., Rezanezhad, F., & Van Cappellen, P. (2017). Solute pools in Nikanotee Fen watershed in the Athabasca oil sands region. *Environmental Pollution*, 225, 150–162. <https://doi.org/10.1016/j.envpol.2017.03.038>
- Smerdon, B. D., Mendoza, C. A., & Devito, K. J. (2007). Simulations of fully coupled lake-groundwater exchange in a subhumid climate with an integrated hydrologic model. *Water Resources Research*, 43, 1–13. <https://doi.org/10.1029/2006WR005137>
- Smerdon, B. D., Mendoza, C. A., & Devito, K. J. (2008). Influence of subhumid climate and water table depth on groundwater recharge in shallow outwash aquifers. *Water Resources Research*, 44(W08427), 1–15. <https://doi.org/10.1029/2007WR005950>
- Soilmoisture Equipment Corp. (2012). *Guelph Permeameter 2800 – Operating Instructions*.
- Spence, C., & Woo, M. (2003). Hydrology of subarctic Canadian shield: soil-filled valleys. *Journal of Hydrology*, 279(1), 151–166. [https://doi.org/10.1016/S0022-1694\(03\)00175-6](https://doi.org/10.1016/S0022-1694(03)00175-6)

- Spennato, H. M., Ketcheson, S. J., Mendoza, C. A., & Carey, S. K. (2018). Water table dynamics in a constructed wetland, Fort McMurray, Alberta. *Hydrological Processes*, *32*(26), 3824–3836. <https://doi.org/10.1002/hyp.13308>
- Strilesky, S. L., Humphreys, E. R., & Carey, S. K. (2017). Forest water use in the initial stages of reclamation in the Athabasca Oil Sands Region. *Hydrological Processes*, *31*(15), 2781–2792. <https://doi.org/10.1002/hyp.11220>
- Sutton, O. F., & Price, J. S. (2019). Soil moisture dynamics modelling of a reclaimed upland in the early post-construction period. *Science of the Total Environment*. <https://doi.org/10.1016/j.scitotenv.2019.134628>
- Thompson, C., Mendoza, C. A., & Devito, K. J. (2017). Potential influence of climate change on ecosystems within the Boreal Plains of Alberta. *Hydrological Processes*, *31*, 2110–2124. <https://doi.org/10.1002/hyp.11183>
- Thompson, C., Mendoza, C. A., Devito, K. J., & Petrone, R. M. (2015). Climatic controls on groundwater – surface water interactions within the Boreal Plains of Alberta: Field observations and numerical simulations. *Journal of Hydrology*, *527*, 734–746. <https://doi.org/10.1016/j.jhydrol.2015.05.027>
- Trites, M., & Bayley, S. E. (2009). Vegetation communities in continental boreal wetlands along a salinity gradient: Implications for oil sands mining reclamation. *Aquatic Botany*, *91*, 27–39. <https://doi.org/10.1016/j.aquabot.2009.01.003>
- Van Huizen, B., Petrone, R. M., Price, J. S., Quinton, W. L., & Pomeroy, J. W. (2020). Seasonal ground ice impacts on spring ecohydrological conditions in a western boreal plains peatland. *Hydrological Processes*, *34*(3), 765–779. <https://doi.org/10.1002/hyp.13626>
- Vitt, D. H., House, M., & Hartsock, J. A. (2016). Sandhill Fen, An Initial Trial for Wetland Species Assembly on In-pit Substrates: Lessons after Three Years. *Botany*, *94*(11), 1015–1025. <https://doi.org/10.1139/cjb-2015-0262>
- Waddington, J. M., Morris, P. J., Kettridge, N., Granath, G., Thompson, D. K., & Moore, P. A. (2014). Hydrological feedbacks in northern peatlands. *Ecohydrology*, *8*(1), 113–127. <https://doi.org/10.1002/eco.1493>
- Weber, M., Bernhardt, M., Pomeroy, J. W., Fang, X., Harer, S., & Schulz, K. (2016). Description of current and future snow processes in a small basin in the Bavarian Alps. *Environmental Earth Sciences*, *75*(17). <https://doi.org/10.1007/s12665-016-6027-1>
- Whittington, P. N., Ketcheson, S., Price, J. S., Richardson, M., & Di Febo, A. (2012). Areal differentiation of snow accumulation and melt between peatland types in the James Bay Lowland. *Hydrological Processes*, *26*, 2663–2671. <https://doi.org/10.1002/hyp.9414>
- Woo, M.-K., & Marsh, P. (2005). Snow, frozen soils and permafrost hydrology in Canada, 1999 – 2002. *Hydrological Processes*, *19*, 215–229. <https://doi.org/10.1002/hyp.5772>
- Woo, M.-K., & Winter, T. C. (1993). The role of permafrost and seasonal frost in the hydrology of northern wetlands in North America. *Journal of Hydrology*, *141*, 5–31.
- Wytrykush, C., Vitt, D. H., Mckenna, G., & Vassov, R. (2012). Designing landscapes to support peatland development of soft tailings deposit - Syncrude Canada Ltd.'s Sandhill Fen Research Watershed initiative. In D. H. Vitt & J. Bhatti (Eds.), *Restoration and Reclamation of Boreal Ecosystems - Attaining Sustainable Development* (pp. 161–178). Cambridge: Cambridge University Press.
- Zhao, L., & Gray, D. M. (1999). Estimating snowmelt infiltration into frozen soils. *Hydrological Processes*, *13*(12–13), 1827–1842.

## TABLES

Table 1. Measured hummock soil properties.

Soil Type	Prescribed Depth	Specific Yield	Porosity	LOI	Bulk Density	$K_{sat}$	Sand <sup>+</sup>	Silt <sup>+</sup>
	cm	-	-	%	g/cm <sup>3</sup>	m/s	%	%
LFH	0 - 15	0.23	0.31	9.3	1.14	1.75E-04	-	-
Pf Sand	15 - 55	0.28	0.23	3.5	1.58	1.09E-04	94	6
Tailings Sand	> 55	0.29	0.26	1.1	1.54	6.74E-05	92	3

<sup>+</sup>(NorthWind Land Resources Inc., 2012)

Table 2. Parameters used to set up CRHM simulations under current and potential climate conditions.

Parameter	Units	Assigned	Module
HRU area	km <sup>2</sup>	3.31E+4 & 1.6E+4	Shared
Aspect	N/E/S/W	S & N	
Elevation	m	318	
Slope	°	8	
Latitude	°	57	
Vegetation height	m	1	
Si (initial soil saturation)	mm <sup>3</sup> mm <sup>-3</sup>	0.2	
Max available water holding capacity	mm	375	
Max values for soil recharge zone	mm	60	
Albedo_bare	-	0.17	Albedo
Albedo_snow	-	0.85	
Groundcover	-	1 (bare ground)	frozenAyers
Soil Texture	-	1 (coarse/medium coarse)	
Soil Temperature	K	271.1	
Coefficient	-	2.82	
Rain_soil_snow	-	1	SnobalCRHM
T_g / G_flux	-	0	
Climate Chg Temp	°C	0, 2, 4, 6	obs
Climate Change Ppt factor	-	1, 1.15, 1.2, 1.3	

Table 3. CRHM simulation results from the frozenAyers module. Variables tested were initial soil saturation (Si), soil temperature (Tsoil) and soil texture.

Si	Runoff	Tsoil	Runoff	Soil Texture	Runoff
-	mm	°C	mm	-	mm
0.2	34	0	Sand	34	
0.25	47	-1	Silt loam	37	
0.3	60	-2	Clay	41	
0.35	72	-4			
0.4	84	-6			
0.45	95	-8			
0.5	105				

Table 4. Summary of CRHM simulation results for projected climate change scenarios. Positive and negative signs indicate if values increased or decreased, respectively from current conditions. Note that values were averaged over the five simulated years (2013-2018).

Climate Scenario	Change in peak snowpack SWE	Change in snow season	Mid-winter melt duration	Mid-winter
2013-2018	%	days	days	mm
T0-P1	0	0	5	12
T2-P1	-21	-10	7	26
T4-P1	-35	-37	14	39
T6-P1	-42	-61	11	43
T0-P1.15	+12	+7	0	0
T0-P1.2	+28	+8	0	0
T0-P1.3	+36	+8	0	0
T2-P1.2	-0.2	-1	6	19
T4-P1.2	-24	-17	12	40
T6-P1.2	-32	-16	14	44

## FIGURE LEGENDS

Graphical Abstract. Runoff was measured directly on constructed hillslopes and is an important freshwater source for wetlands in a sub-humid and saline environment.

Figure 1. Instrumentation map of Sandhill Fen Watershed. Dark grey areas represent the lowland (wetland) area and lighter grey represents the margins and upland areas. Circles represent snow survey points which are coloured based on landscape type. The “V” shape at the base of the runoff collectors indicate the physical constructed boundary and thinner lines represent the calculated upslope contributing areas.

Figure 2. Runoff collector construction phases. a) Two 10-15 cm trenches were dug into the frozen ground, b) hydraulic cement was used to seal the garden edging into the trenches, c) trenches tapered at the bottom of the slope to form a “V” where an eavestrough was used to funnel water towards the bucket with a v-notch, d) a pressure transducer was used to continuously measure water height and discharge, e) completed runoff collector where each arm of the “V” was ~4 m.

Figure 3. Boxplots of snowpack SWE prior to melt in a) landscape units and b) hummock slope position and aspect. Circular points are data points from the snow surveys. Outer border of the boxplots represent the 25<sup>th</sup> and 75<sup>th</sup> percentiles and mid box lines represent the group median. The diamond points represent the group mean and numbers above the x-axis indicate sample size. Means sharing a letter are not significantly different (Wilcoxon rank sum test).

Figure 4. Snowpack SWE of each landscape unit from before and during melt for the a) wetland, b) upland, c) hummocks and d) hummock aspects. The data points represent the mean SWE and the top and bottom of the shaded areas represent the 75<sup>th</sup> and 25<sup>th</sup> percentiles, respectively.

Figure 5. Snowmelt runoff collector discharge (cm<sup>3</sup>/s) and cumulative runoff (mm) at 15-minute intervals for two distinct melt periods of a) South-facing runoff collector from 15-22 March 2018 and b) North-facing collector during 12-24 April 2018. Note: 1) figure scales are different and 2) the entire snowpack had melted by the end of each melt period shown.

Figure 6. Observed and CRHM simulated a) hourly snowpack SWE from 2013-2018 and b) daily snowmelt surface runoff for the 2017-2018 winter season.

Figure 7. Simulated SWE under climate scenarios of a) increased temperature (T2-P1, T4-P1, T6-P1), b) increased precipitation (T0-P1.5, T0-P1.2, T0-P1.3) and c) increased temperature and precipitation (T2-P1.2, T4-P1.2, T6-P1.2). The black dotted line is the simulated SWE under current climate conditions (T0-P1).

Figure 8. Simulated snowmelt runoff under climate scenarios of a) increased temperature (T2-P1, T4-P1, T6-P1), b) increased precipitation (T0-P1.5, T0-P1.2, T0-P1.3) and c) increased temperature and precipitation (T2-P1.2, T4-P1.2, T6-P1.2). The dark grey bar represents the simulated runoff under current climate conditions (T0-P1).

Figure 9. Average SWE of older constructed systems on the Syncrude Canada Ltd. property. Data points represent daily average SWE data from snow surveys conducted during the 2017-2018 winter. Inset: photographs to indicate maturity differences among sites for South Bison (SB), Coke Beach (CB), Jake Pine (JP) and Sandhill Fen Watershed (SFW).

## APPENDIX

Table A1. All simulation results from the Cold Regions Hydrological Model under current and various potential future climate scenarios.

Climate Scenario	Simulation Results
<b>Scenario</b>	<b>Temperature Increase</b>
°C	mm/day
T0-P1	0
2014-2015	22-Nov-14
2015-2016	15-Nov-15
2016-2017	27-Nov-16
2017-2018	19-Nov-17

T2-P1	2
2014-2015	21-Nov-14
2015-2016	15-Nov-15
2016-2017	27-Nov-16
2017-2018	19-Nov-17
T4-P1	4
2014-2015	21-Nov-14
2015-2016	23-Jan-16
2016-2017	27-Nov-16
2017-2018	19-Nov-17
T6-P1	6
2014-2015	21-Nov-14
2015-2016	23-Jan-16
2016-2017	27-Nov-16
2017-2018	19-Nov-17
T0-P1.15	0
2014-2015	22-Nov-14
2015-2016	15-Nov-15
2016-2017	27-Nov-16
2017-2018	19-Nov-17
T0-P1.2	0
2014-2015	21-Nov-14
2015-2016	15-Nov-15
2016-2017	27-Nov-16
2017-2018	19-Nov-17
T0-P1.3	0
2014-2015	21-Nov-14
2015-2016	15-Nov-15
2016-2017	26-Nov-16
2017-2018	19-Nov-17
T2-P-1.2	2
2014-2015	21-Nov-14
2015-2016	15-Nov-15
2016-2017	27-Nov-16
2017-2018	19-Nov-17
T4-P1.2	4
2014-2015	21-Nov-14
2015-2016	8-Dec-15
2016-2017	27-Nov-16
2017-2018	19-Nov-17
T6-P1.2	6
2014-2015	22-Nov-14
2015-2016	23-Jan-16
2016-2017	27-Nov-16
2017-2018	19-Nov-17

---

<sup>+</sup>Sum of two mid-winter melt events

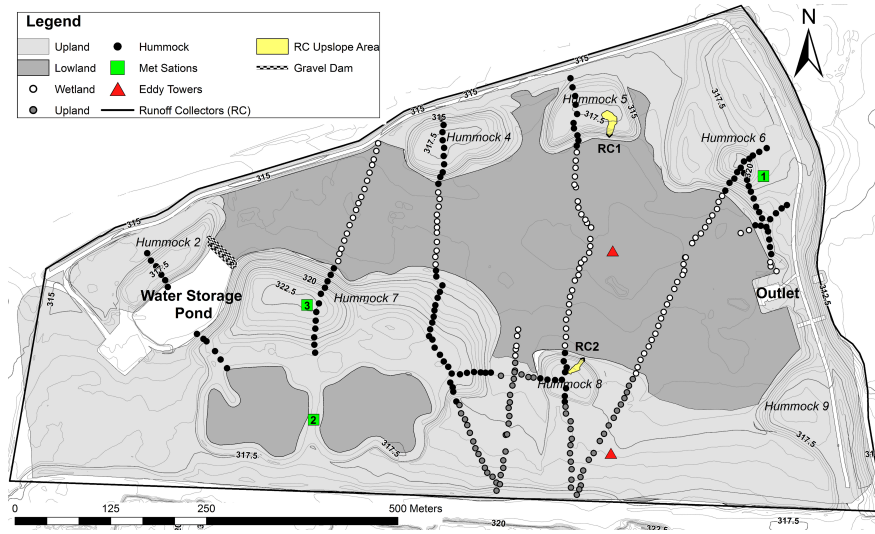


Figure 1: Figure 1. Instrumentation map of Sandhill Fen Watershed. Dark gray areas represent the lowland (wetland) area and lighter grey represents the margins and upland areas. Circles represent snow survey points which are coloured based on landscape type. The “V” shape at the base of the runoff collectors indicate the physical constructed boundary and thinner lines represent the calculated upslope contributing areas.

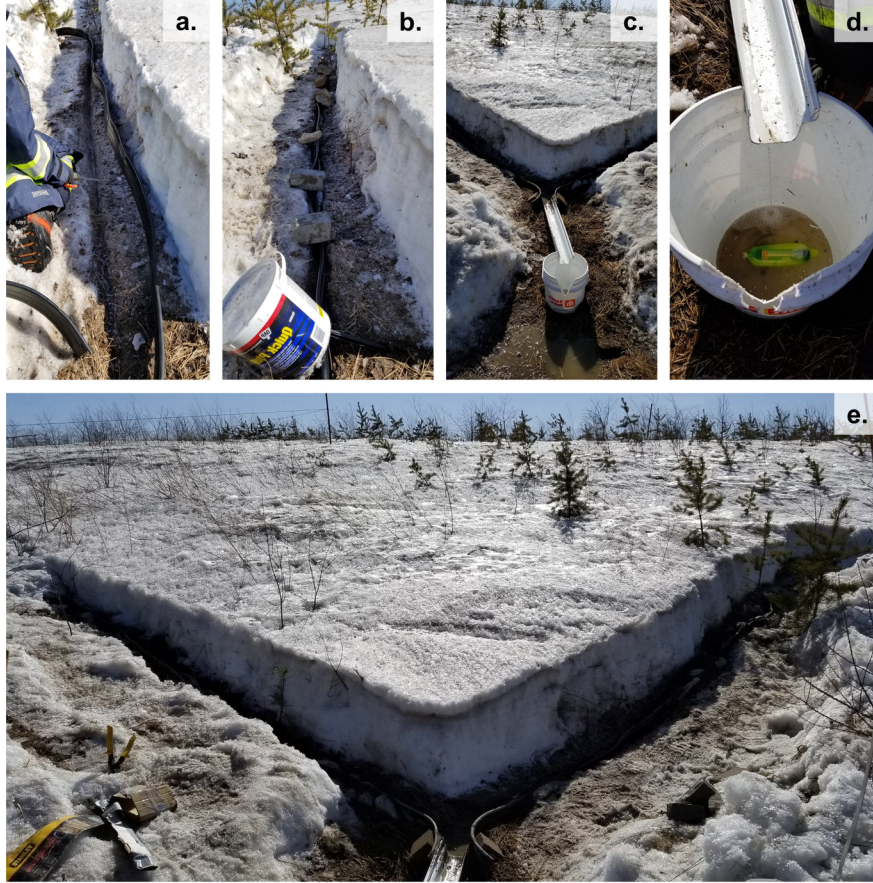


Figure 2: Figure 2. Runoff collector construction phases. a) Two 10-15 cm trenches were dug into the frozen ground, b) hydraulic cement was used to seal the garden edging into the trenches, c) trenches tapered at the bottom of the slope to form a “V” where an eavestrough was used to funnel water towards the bucket with a v-notch, d) a pressure transducer was used to continuously measure water height and discharge, e) completed runoff collector where each arm of the “V” was  $\sim 4\text{m}$ .

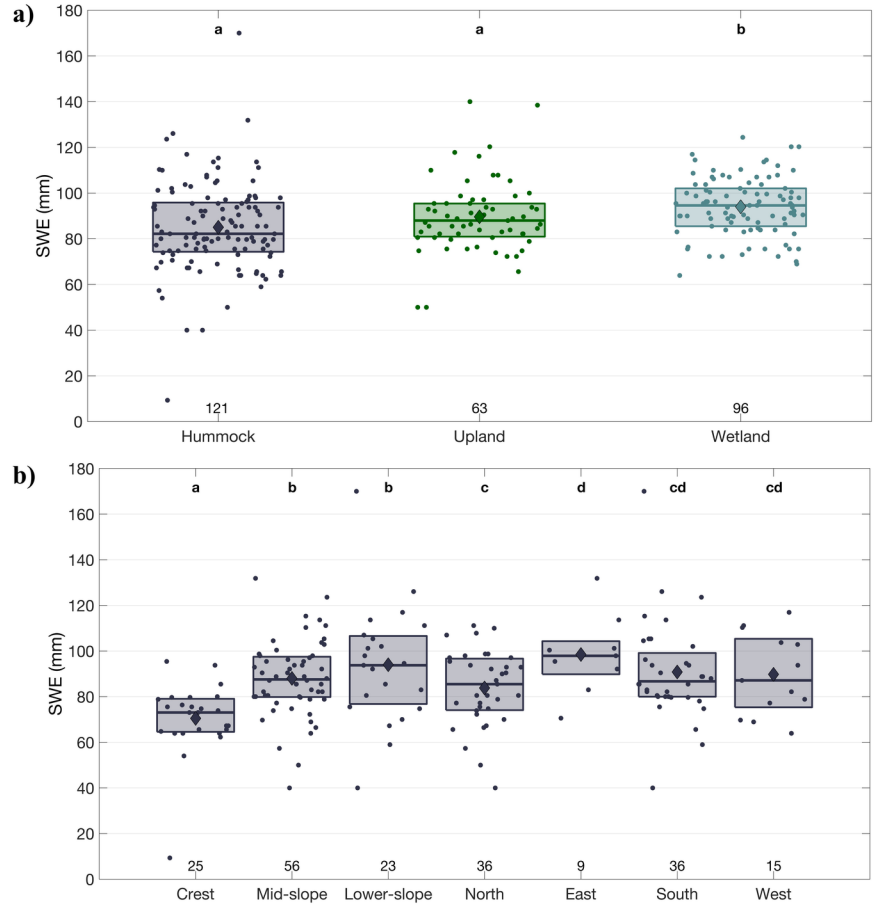


Figure 3: Figure 3. Boxplots of snowpack SWE prior to melt in a) landscape units and b) hummock slope position and aspect. Circular points are data points from the snow surveys. Outer border of the boxplots represent the 25th and 75th percentiles and mid box lines represent the group median. The diamond points represent the group mean and numbers above the x-axis indicate sample size. Means sharing a letter are not significantly different (Wilcoxon rank sum test).

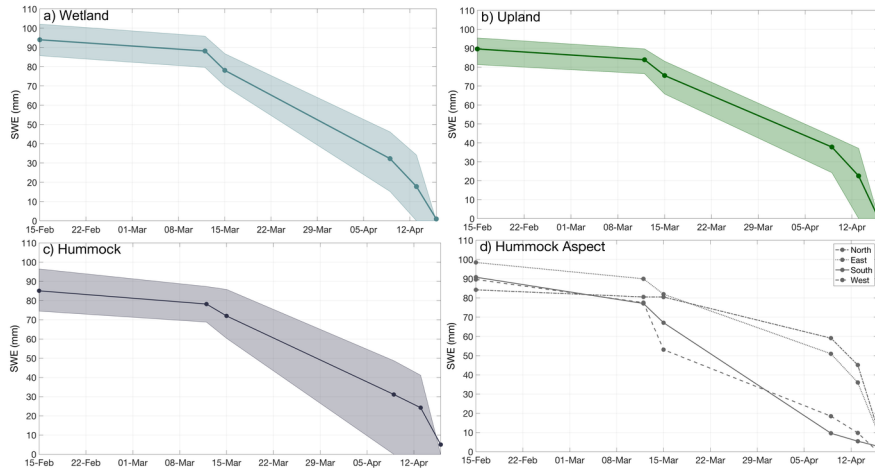


Figure 4: Figure 4. Snowpack SWE of each landscape unit from before and during melt for the a) wetland, b) upland, c) hummock and d) hummock aspects. The data points represent the mean SWE and the top and bottom of the shaded areas represent the 75th and 25th percentiles, respectively.

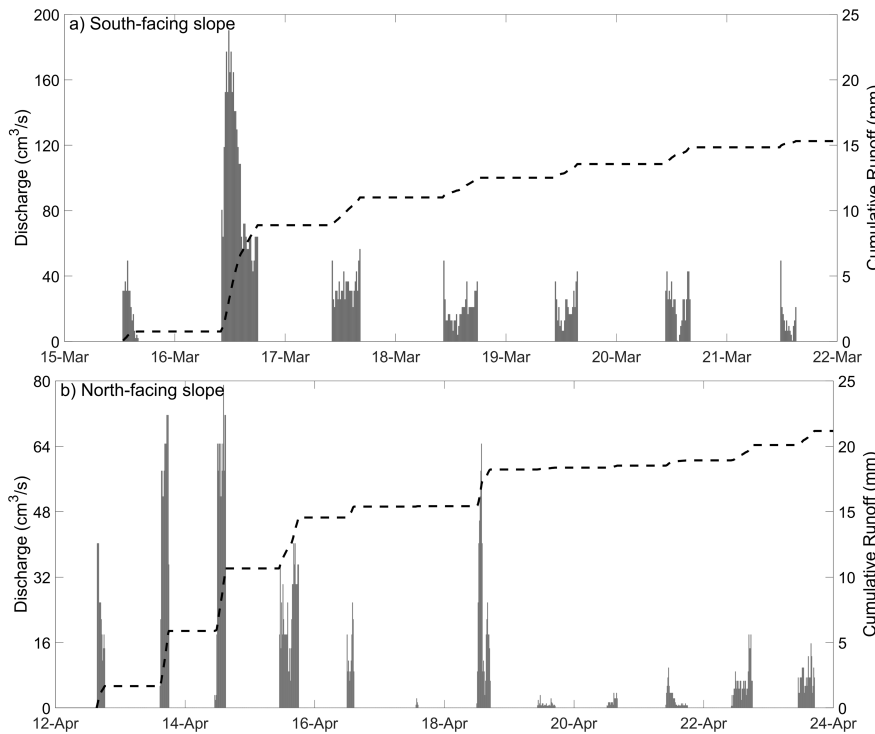


Figure 5: Figure 5. Snowmelt runoff collector discharge ( $\text{cm}^3/\text{s}$ ) and cumulative runoff (mm) at 15-minute intervals for two distinct melt periods of a) South-facing runoff collector from 15-22 March 2018 and b) North-facing collector during 12-24 April 2018. Note: 1) figure scales are different and 2) the entire snowpack had melted by the end of each melt period shown.

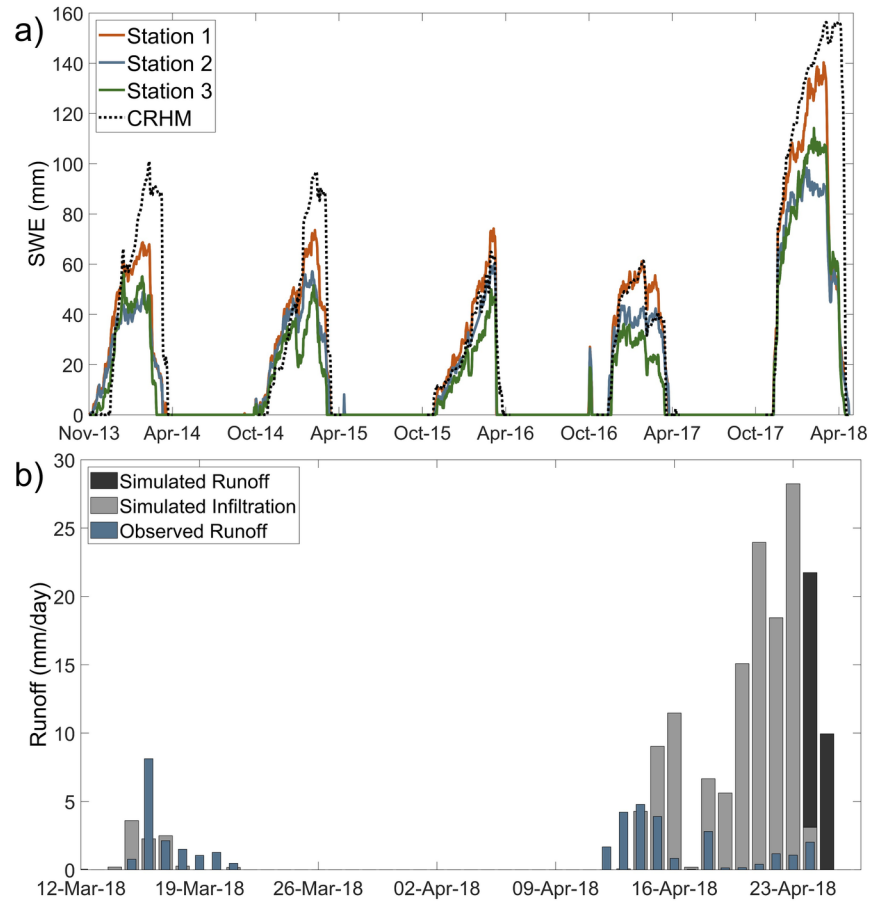


Figure 6: Figure 6. Observed and CRHM simulated a) hourly snowpack SWE from 2013-2018 and b) daily snowmelt surface runoff for the 2017-2018 winter season.

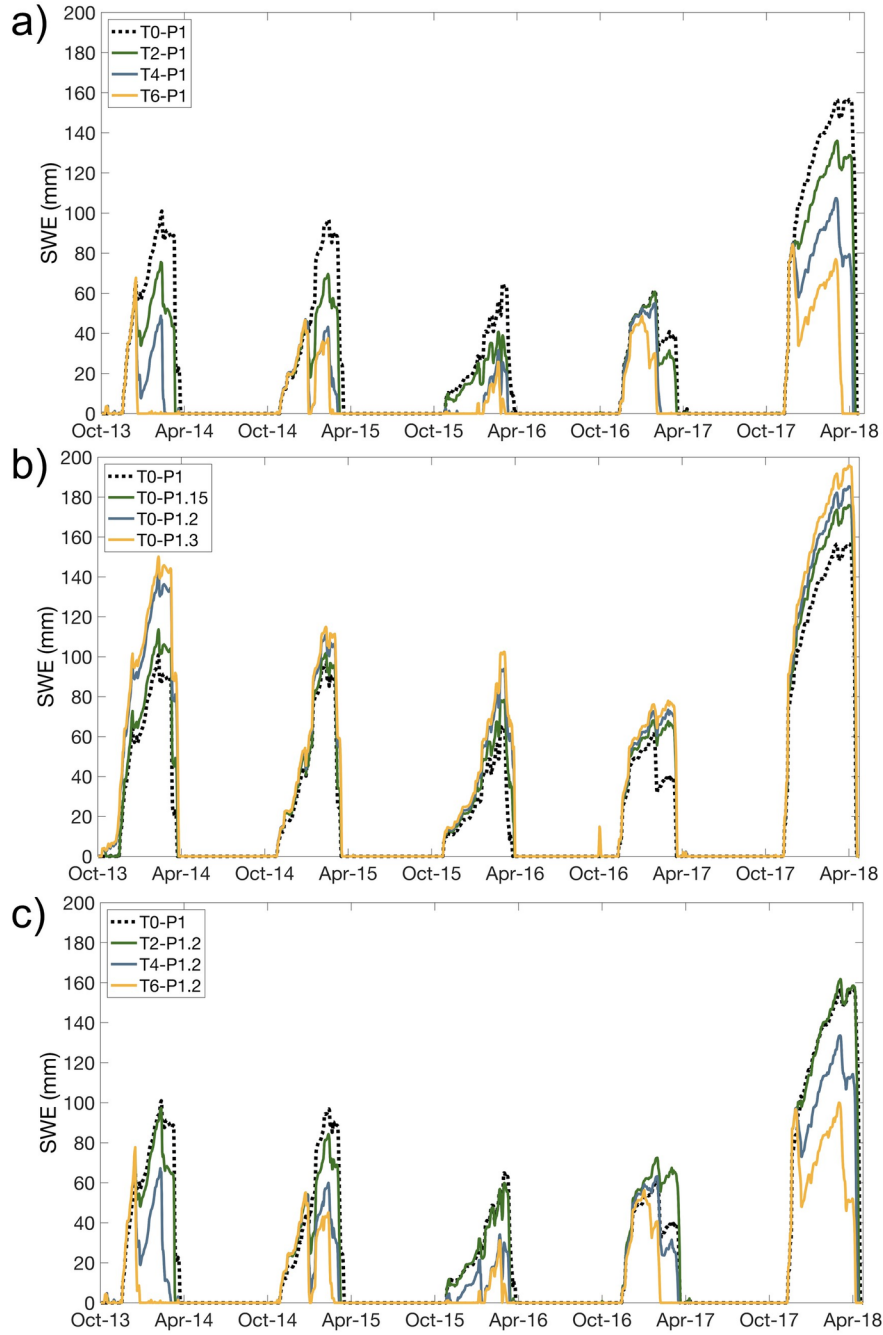


Figure 7: Figure 7. Simulated SWE under climate scenarios of a) increased temperature (T2-P1, T4-P1, T6-P1), b) increased precipitation (T0-P1.5, T0-P1.2, T0-P1.3) and c) increased temperature and precipitation (T2-P1.2, T4-P1.2, T6-P1.2). The black dotted line is the simulated SWE under current climate conditions (T0-P1).

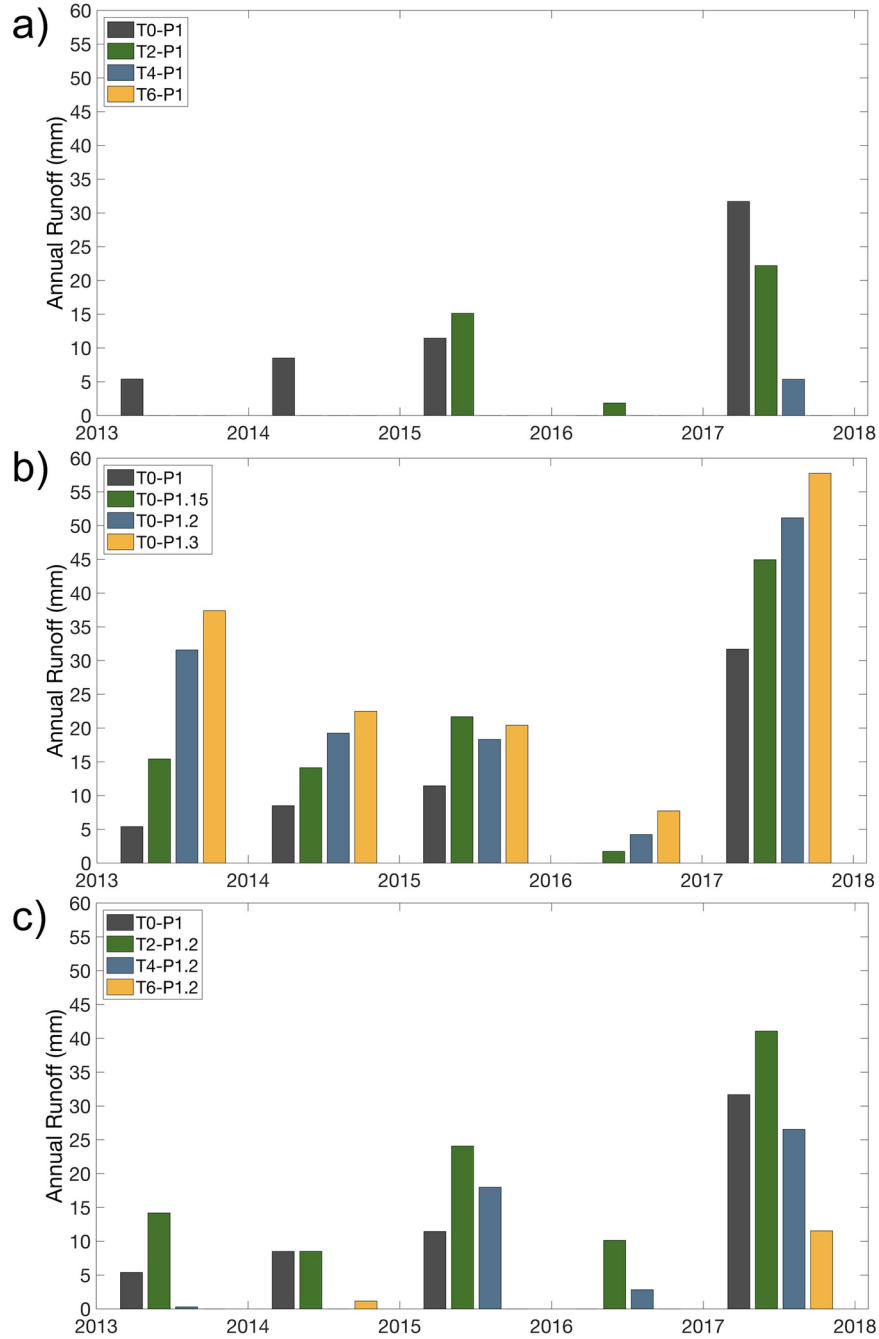


Figure 8: Figure 8. Simulated snowmelt runoff under climate scenarios of a) increased (T2-P1, T4-P1, T6-P1), b) increased precipitation (T0-P1.5, T0-P1.2, T0-P1.3) and c) increased temperature and precipitation (T2-P1.2, T4-P1.2, T6-P1.2). The dark grey bar represents the simulated runoff under current climate conditions (T0-P1).

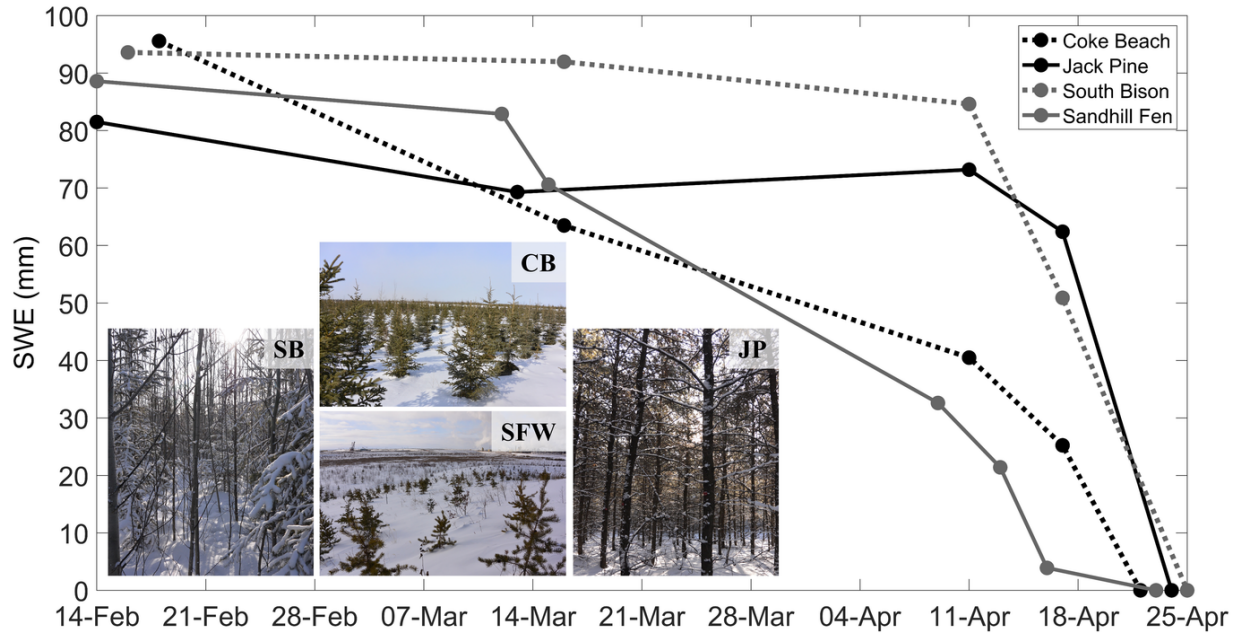


Figure 9: Figure 9. Average SWE of older constructed systems on the Syncrude Canada Ltd. property. Data points represent daily average SWE data from snow surveys conducted during the 2017-2018 winter. Inset: photographs to indicate maturity differences among sites for South Bison (SB), Coke Beach (CB), Jack Pine (JP), and Sandhill Fen Watershed (SFW).